EXPERIENCE OF FIELD MEASUREMENT AND COMPUTER SIMULATION METHODS FOR PILLAR DESIGN

By Winton J. Gale, Ph.D.[1]

ABSTRACT

Coal pillar design has been based on generalized formulas of the strength of the coal in a pillar and experience in localized situations. Stress measurements above and in coal pillars indicate that the actual strength and deformation of pillars vary much more than predicted by formulas. This variation is due to failure of strata surrounding coal. The pillar strength and deformation of the adjacent roadways is a function of failure in the coal and the strata about the coal. When the pillar is viewed as a system in which failure also occurs in the strata rather than the coal only, the wide range of pillar strength characteristics found in the United Kingdom, United States, Republic of South Africa, Australia, People's Republic of China, Japan, and other countries are simply variations due to different strata-coal combinations, not different coal strengths.

This paper presents the measured range of pillar strength characteristics and explains the reasons. Methods to design pillar layouts with regard to the potential strength variations due to the strata strength characteristics surrounding the seam are also presented.

[1]Managing director, Strata Control Technology, Wollongong East, New South Wales, Australia.

INTRODUCTION

The strength characteristics of coal pillars have been studied by many, and the subject is well discussed in the literature (Salamon and Munro [1967]; Wilson [1972]; Hustrulid [1976]; Mark and Iannacchione [1992]; Gale [1996]). In general, a range of strength relationships has been derived from four main sources:

(1) Laboratory strength measurements on different-sized coal block specimens;
(2) Empirical relationships from observations of failed and unfailed pillars;
(3) A theoretical fit of statistical data and observations; and
(4) Theoretical extrapolation of the vertical stress buildup from the ribside toward the pillar center to define the load capacity of a pillar.

These relationships provide a relatively wide range of potential strengths for the same pillar geometry. In practice, it has been found that various formulas are favored (or modified) by users, depending on past experience in their application to certain mining districts or countries.

In general, the application of empirically and statistically based formulas has been restricted to the mining method and geological environment for which they were developed, and they often relate to specific pillar geometries. In general, these methods were developed for shallow, extensive bord-and-pillar operations for which the pillar was designed to hold the weight of overburden. The wider application of longwall mining methods and increasing depth has required a greater understanding of factors influencing pillar strength and their role in the control of ground deformation about the mining operations. The development of stress measurement and detailed rock deformation recording tools over the last 10-15 years has allowed much more quantification of actual pillar stresses and deformations. Few data were available when many of the pillar strength relationships were originally defined. Similarly, the development of computer simulation methods has allowed detailed back-analysis of the mechanics of strata-coal interaction in formed-up pillars.

The author and his colleagues have conducted numerous monitoring and stress measurement programs to assess roadway stability and pillar design requirements in Australia, the United Kingdom, Japan, the United States, Indonesia, and Mexico. The results of these investigations and others reported in the literature have demonstrated that the mechanical response of the coal and surrounding strata defines the pillar strength, which can vary widely depending on geology and stress environment. The application of a pillar strength formula to assess the strength of a system that is controlled by the interaction of geology, stress, and associated rock failure is commonly an oversimplification.

MECHANICS OF THE PILLAR-COAL SYSTEM

The strength of a pillar is determined by the magnitude of vertical stress that can be sustained within the strata-coal sequence forming and bounding it. The vertical stress developed through this sequence can be limited by failure of one or more of the units that comprise the pillar system. This failure may occur in the coal, roof, or floor strata forming the system, but usually involves the coal in some manner. The failure modes include shear fracture of intact material, lateral shear along bedding or tectonic structures, and buckling of cleat-bounded ribsides.

In pillar systems with strong roof and floor, the pillar coal is the limiting factor. In coal seams surrounded by weak beds, a complex interaction of strata and coal failure will occur; this will determine the pillar strength. The strength achievable in various elements largely depends on the confining stresses developed, as illustrated in figure 1. This indicates that as confinement is developed in a pillar, the axial strength of the material increases significantly, thereby increasing the actual strength of the pillar well above its unconfined value.

The strength of the coal is enhanced as confining stress increases toward the pillar center. This increased strength is often related to the width-to-height (w/h) ratio; the larger the ratio, the greater the confinement generated within the pillar. Hence, squat pillars (high w/h) have greater strength potential than slender ones (low w/h).

The basic concepts related to confinement within coal pillars were developed by Wilson [1972]; with the growing availability of measurement data, these general mechanics are widely accepted. However, confining stress can be reduced by roadway deformations such as floor heave, bedding plane slip, and other failure mechanisms. These mechanisms are described below.

ROADWAY DEVELOPMENT PHASE

Prior to mining, the rock and coal units will have in situ horizontal and vertical stresses that form a balanced initial stress state in the ground. As an opening (roadway) is created in a coal seam, there is a natural tendency for the coal and rock to move laterally and vertically into the roadway. In this situation, the horizontal stress acting across the pillar will form the confining stress within that pillar. If this lateral displacement is resisted by sufficient friction, cohesion, and shear stiffness of the immediate roof and floor layers, then most of the lateral confining stress is maintained within the pillar. Consequently, the depth of "failure" (yield) into the pillar ribside is small. If the coal and rock layers are free to move into the roadways by slippage along bedding planes or shear deformation of soft bands, this confining stress will be reduced.

Hence, the depth of failure into the pillar ribside may be significantly greater.

The geometry of failure in the system and the residual strength properties of the failure planes will therefore determine the nature of confining stress adjacent to the ribsides and extending across the pillars. This mechanism determines the depth of failure into the pillar and the extent of ribside displacement during roadway drivage.

PILLAR LOADING BY ABUTMENT STRESSES

Roadways are subjected to an additional phase of loading during longwall panel extraction, as front and then side abutment pressures are added to the previous (and generally much smaller) stress changes induced by roadway excavation. These abutment stresses typically considered are predominantly vertical in orientation, but can generate additional horizontal (confining) stresses (by the Poisson's ratio effect) if there is sufficient lateral restraint from the surrounding roof and floor. Conversely, if the ground is free to move into the roadway, this increased horizontal stress is not well developed and increased rib squeeze is manifest instead.

This concept is presented in figure 2; with strong cohesive coal-rock interfaces the confining stress in the pillar increases rapidly inward from the ribsides, allowing high vertical stresses to be sustained by the pillar. The opposite case of low shear strength coal-rock contact surfaces is presented in figure 3. In this situation, confinement cannot be maintained sufficiently; hence, the allowable vertical stress would be significantly less than that in figure 2. The diagram shows that the pillar has failed because of its inability to sustain the imposed vertical abutment stresses. In addition, lateral movement has caused floor heave and severe immediate roof shearing.

The implications of this for the strength of an isolated pillar are presented in figure 4, where the load carried by the pillar is the mean of the vertical stress across it. If this mean stress is equal to the average "applied load" to be carried by the pillar, then the pillar is stable (figure 4*A*). If the applied load is greater, then the pillar is said to fail (figure 4*B*) and the deficit stress must be redistributed onto nearby pillars.

Conceptually, pillar strength behavior should fall between the two end members of:

(1) Lateral slip occurring totally unresisted, so that pillar strength is limited to the unconfined value of the coal; and

(2) Lateral slip being resisted by system cohesion and stiffness, such that pillar strength is significantly above its unconfined value due to confinement.

A range of potential pillar strengths associated with these two end members relative to the w/h ratio is presented after Gale [1996] in figure 5. It is assumed that the rock mass strength of the coal is 6.5 MPa and that the coal is significantly involved in the failure process. This range of pillar strengths is representative of most rock failure combinations, except in rare cases where small stiff pillars may punch into soft clay-rich strata at loading levels below the field uniaxial compressive strength of the coal. In the punching situations, pillar strength may be lower than that depicted, but the variation would generally be confined to pillars having small w/h ratios.

A comparison of these "end member" situations with a range of pillar strengths determined from actual measurement programs conducted in Australia and the United Kingdom by Strata Control Technology and from the United States [Mark

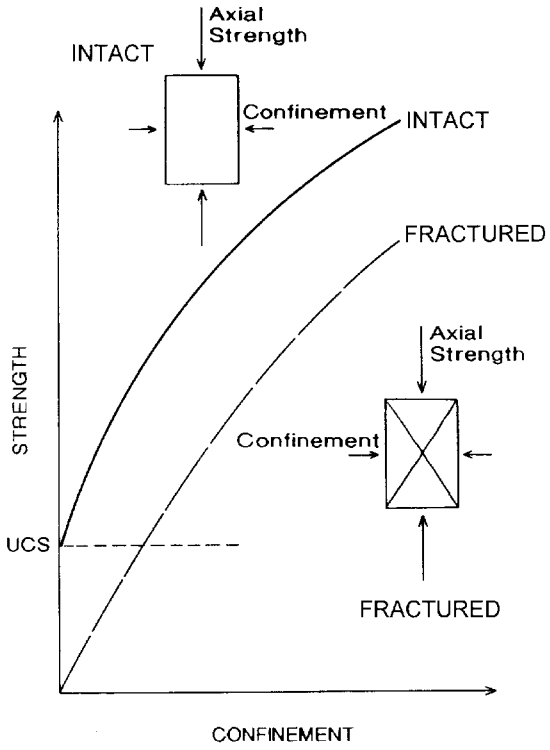

Figure 1.—Effect of confining stress on compressive strengths of intact and fractured rocks.

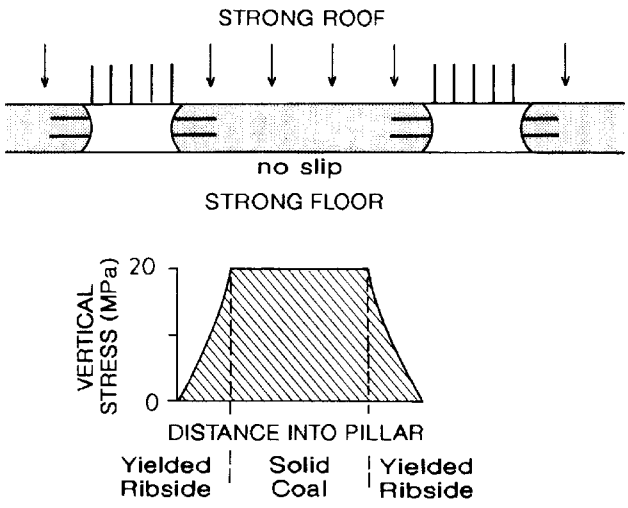

Figure 2.—Rapid buildup of vertical stress into the pillar where high confining stresses are maintained.

et al. 1988] is presented in figure 6. The comparison indicates that a wide range of pillar strengths have been measured for the same geometry (in terms of w/h) and that the data appear to span the full interval between the end members. However, two groupings can be discerned and are shaded in figure 7:

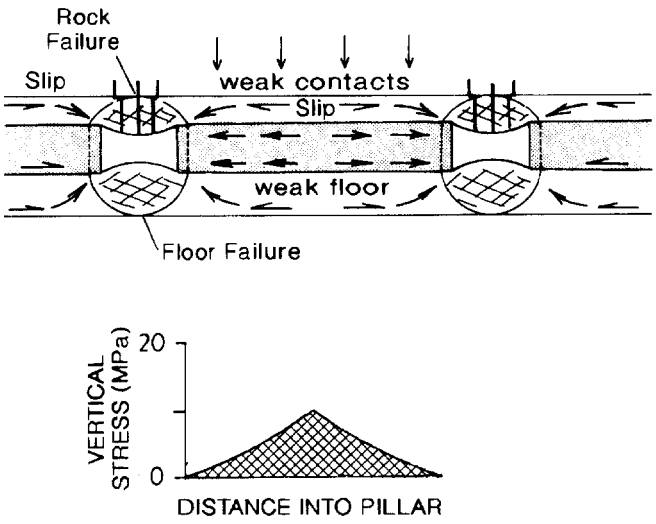

Figure 3.—Slow buildup of vertical stress in the pillar where slip occurs and confinement is reduced.

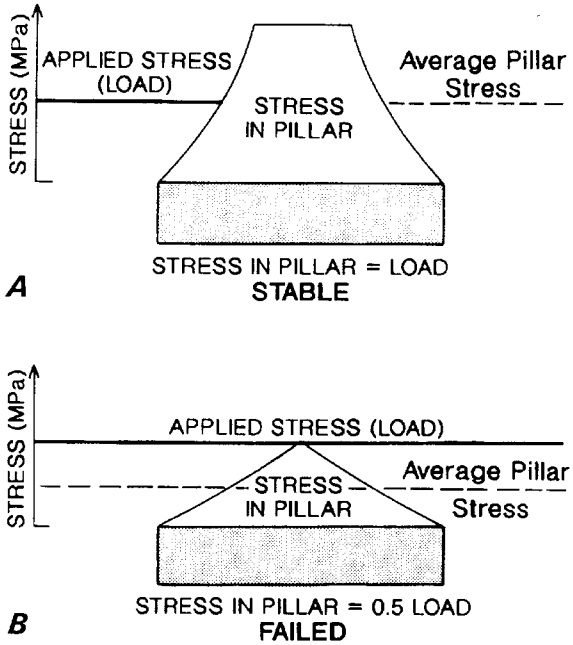

Figure 4.—Pillar strength cases for strong and weak geologies. *A*, strong system; *B*, weak system.

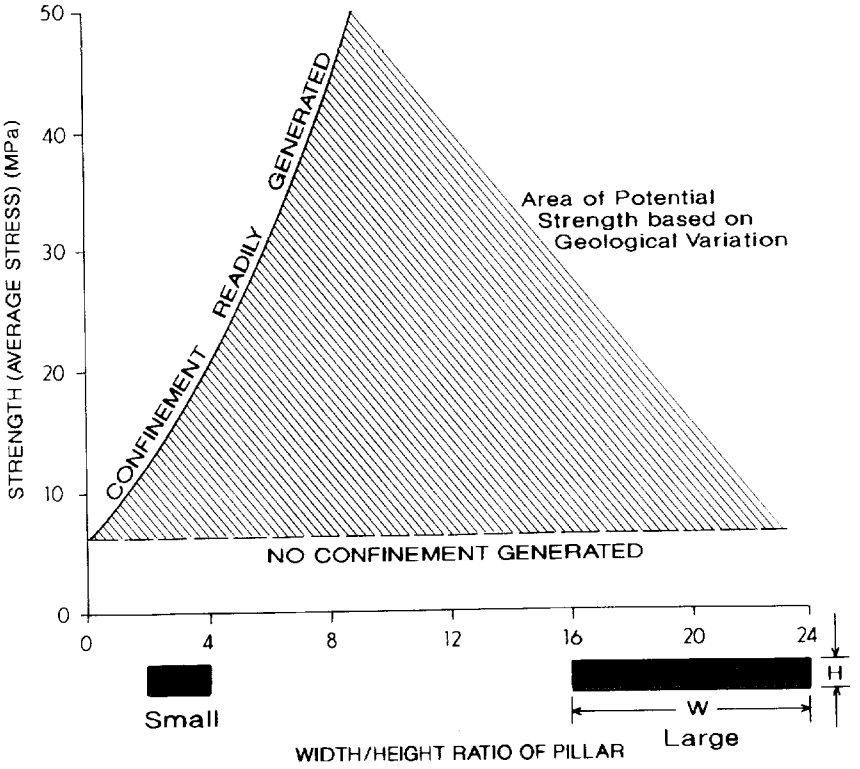

Figure 5.—Range of potential pillar strengths relative to w/h based on confinement variation (after Gale [1996]).

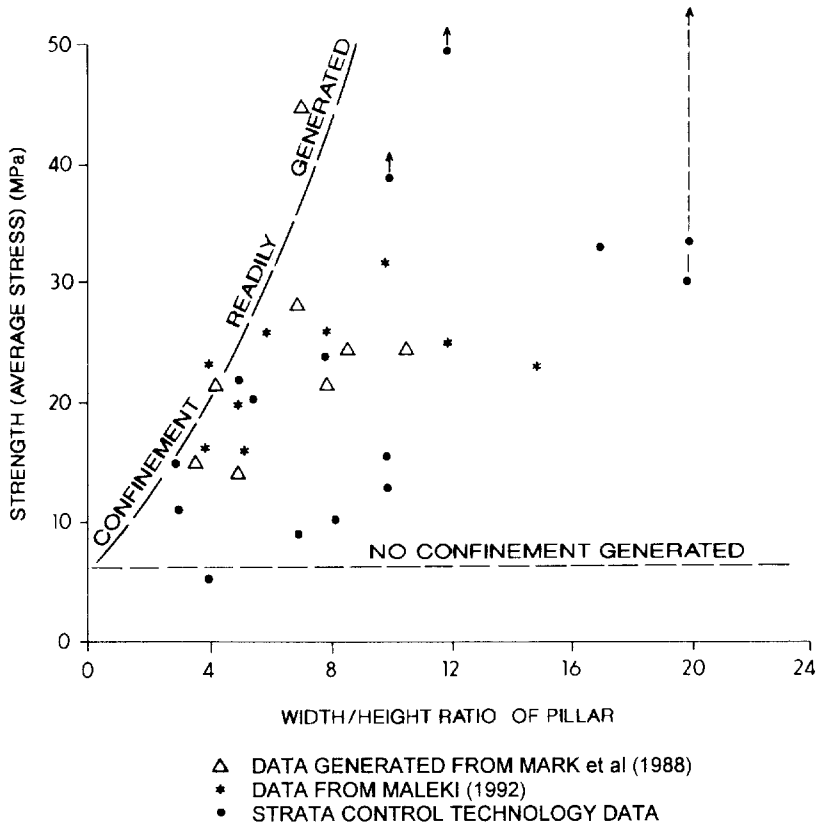

Figure 6.—Pillar strength information relative to changes (after Gale [1996]).

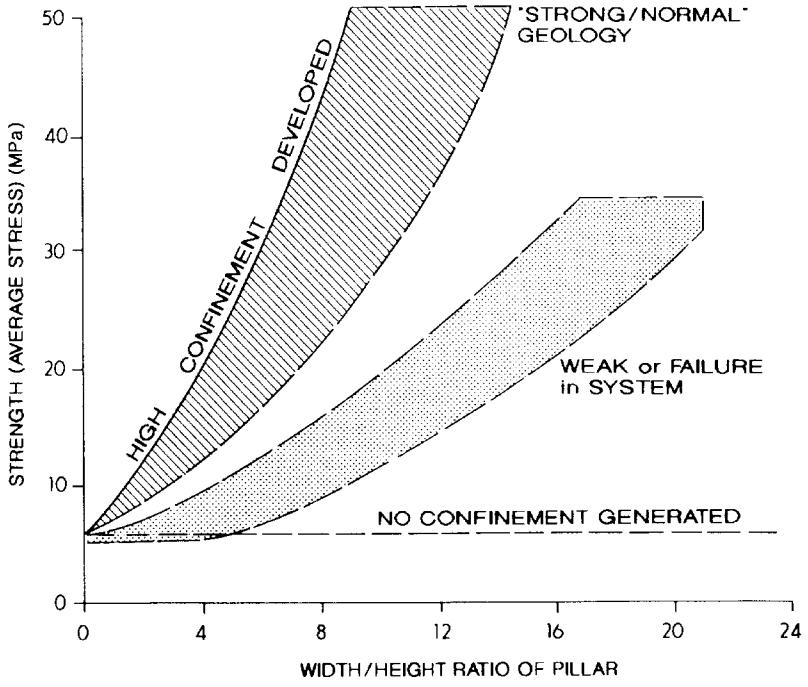

Figure 7.—Generalized groupings of strong/normal and weak geology (after Gale [1996]).

(1) The "strong/normal" geologies, where pillar strength appears to be close to the upper bound.

(2) The structured or weak geologies, where the strength is closer to the lower bound and it is apparent that the strength of the system is significantly limited.

It should be noted that these two groupings are arbitrary and are possibly due to limited data. With more data points, the grouping may become less obvious.

EFFECT OF GEOLOGY

It is clear that a wide range of pillar strengths is possible and that these are not only related to coal strength and w/h ratio. Geological factors have a major impact on the strength achievable under the various pillar geometries.

EFFECT OF GEOLOGY ON PILLAR STRENGTH

The effect of various strata types in the roof-coal-floor pillar systems has been investigated further by computational methods. Computer models of four pillar systems were loaded to determine their strength characteristics (figure 8). These are—

- Massive sandstone-coal-massive sandstone
- Laminite-coal-sandstone
- Weak siltstone-coal-weak siltstone
- Laminite-clayband-coal-clayband-laminite

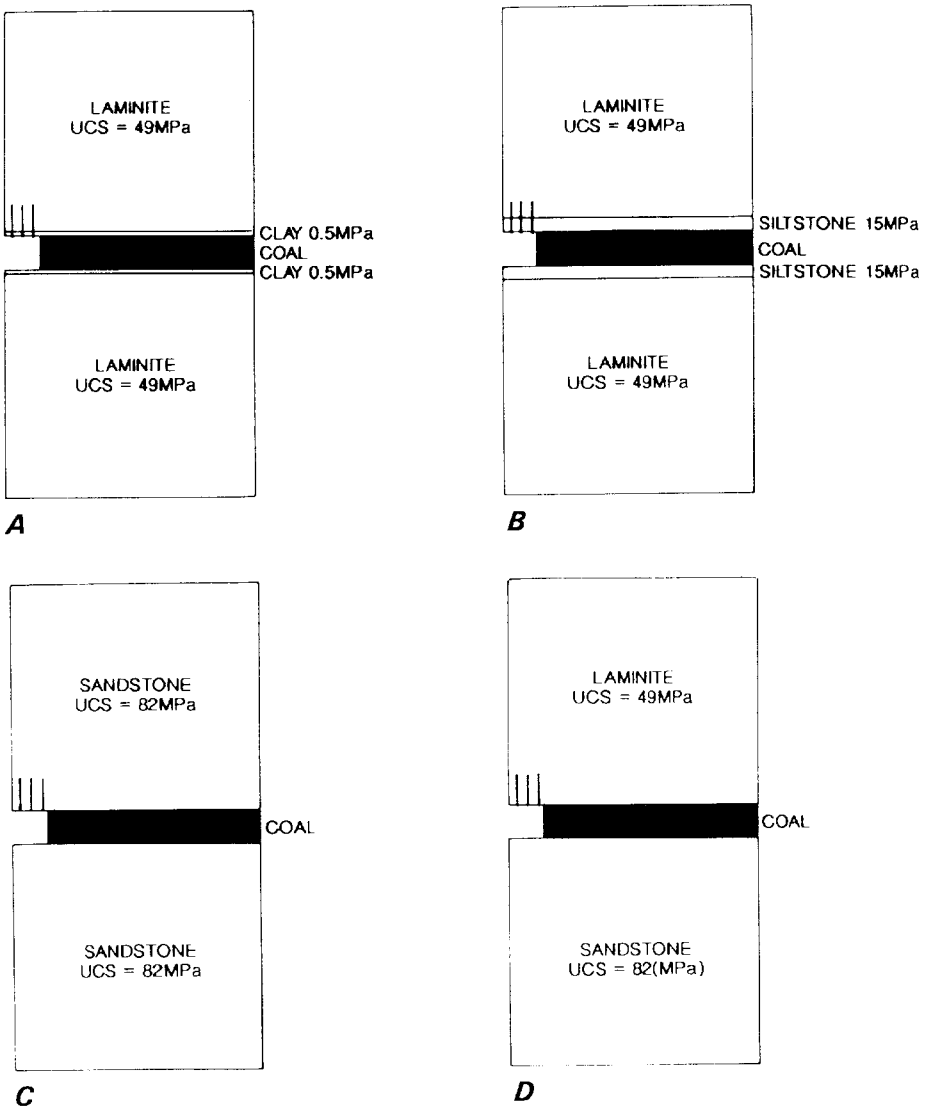

Figure 8.—Geological sections modeled to assess load deformation characteristics. *A*, coal-clay-laminite; *B*, coal-siltstone-laminite; *C*, coal-sandstone; *D*, coal-laminite-sandstone.

The results of the pillar strength characteristics relative to w/h are presented in figure 9. The results closely relate to the field measurement data and confirm that the strata types surrounding the coal have a major impact on strength and also provide insight into the geological factors affecting strength. The results indicate that—

(1) Strong immediate roof and floor layers and good coal-to-rock contacts provide a general relationship similar to the upper bound pillar strength in figure 5.

(2) Weak, clay-rich, and sheared contacts adjacent to the mining section reduce pillar strength to the lower bound areas.

(3) Soft strata in the immediate roof and floor, which fail under the mining-induced stresses, will weaken pillars to the lower bound areas.

(4) Tectonic deformation of coal in disturbed geological environments will reduce pillar strength, although the extent depends on geometry and strength of the discontinuities.

Obviously, combinations of these various factors will have a compounding effect. For example, structurally disturbed, weak, and wet roof strata may greatly reduce pillar confinement and, consequently, pillar-bearing capacity.

EFFECT OF GEOLOGY ON POSTPEAK PILLAR STRENGTH

The postpeak pillar strength characteristics for some of the pillars modeled are presented in figure 10. The pillar strength is presented as a stress/strain plot for various width/height pillars. The results presented in figure 10*A* show that in strong sandstone geology, high strengths are achievable in small pillars (w/h ' 5) and the pillar maintains a high load-carrying capability. In the example modeled, "short-term" load losses were noted to occur in association with sudden rib failure. These instances are present in figure 10*A* as "rib bumps." In sections of laminite roof, these pillars may lose strength if the laminite fails at a very high load above the pillar. For pillars with a w/h less than 4/5, a loss in strength is expected at a high load due to failure of the coal.

In pillar systems with weak strata surrounding the coal, the pillars typically exhibit a strength loss after peak load is achieved. Large width/height pillars are required to develop a high load-carrying capacity after failure in the weak pillar systems modeled. Two examples are presented in figure 10*B*, which shows the postpeak strength characteristics of pillars with weak mudstone or clay surrounding the coal. In these

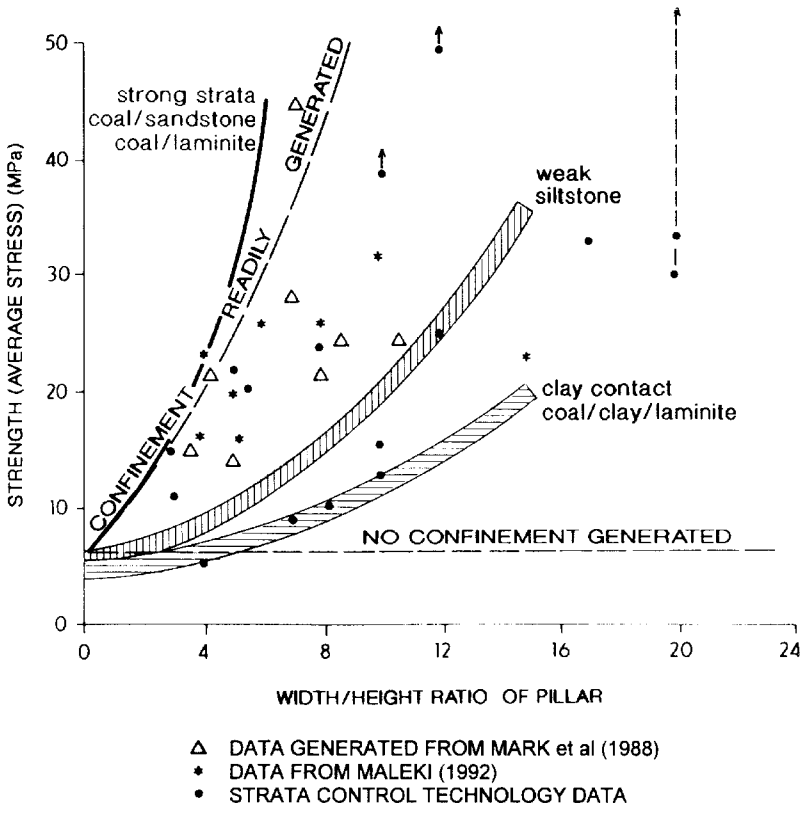

Figure 9.—Strength and w/h for models.

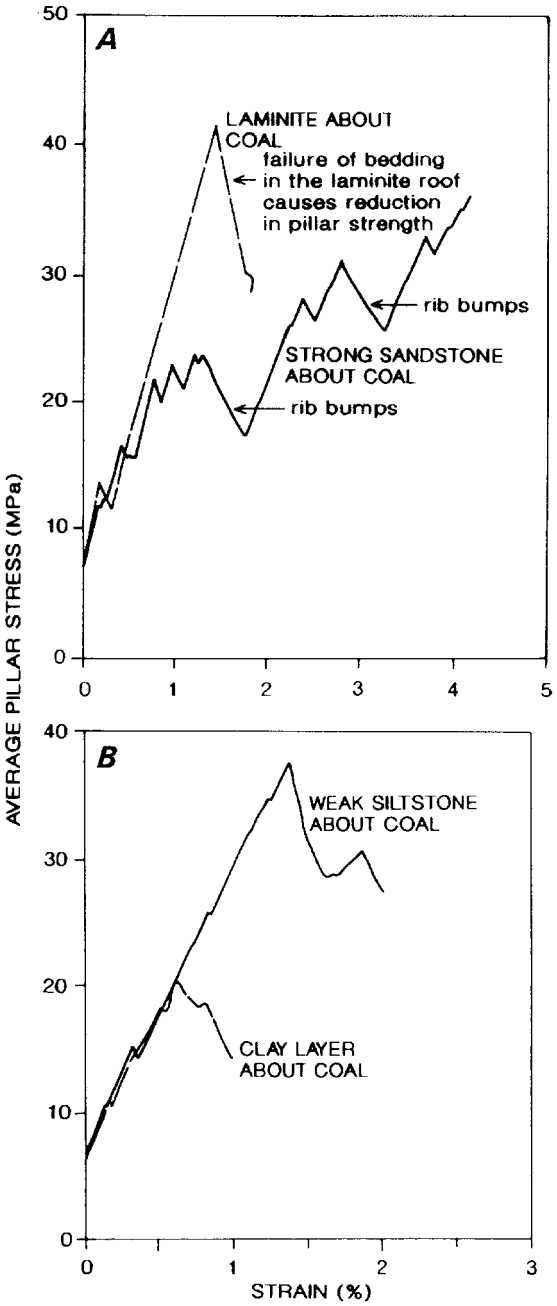

Figure 10.—Postpeak strength of models. *A*, w/h ' 5; *B*, w/h ' 15.

examples, the strength loss is greater in the situation of weak clay surrounding the coal.

The implications of this are significant for the design of barrier and chain pillars where high loads are anticipated. If excessive loads are placed on development pillars in this environment, pillar creep phenomena are possible due to the load shedding of failed pillars sequentially overloading adjacent pillars. The effect of load shedding in chain pillars when isolated in the goaf is to redistribute load onto the tailgate area and to potentially display increased subsidence over the pillar area. The typical result is to have major tailgate deformation, requiring significant secondary support to maintain access and ventilation.

AN APPROACH TO PILLAR DESIGN

Field studies suggest that a range of strengths is possible extending within upper and lower bounds. If we make use of these relationships as "first-pass estimates" to be reviewed by more detailed analysis later, then a number of options are available. In known or suspected weak geologies, the initial design may utilize the lower bound curve of the weak geology band in figure 7. In good or normal geologies, the Bieniawski or squat pillar formulas may be suitable for initial estimates. Two obvious problems with this approach are:

(1) Estimates of pillar size can vary greatly, depending on the geological environment assumed; and

(2) The pillar size versus strength data set used (figure 6) is limited.

This is why such formulas or relationships are considered as first-pass estimates only, to be significantly improved later by more rigorous site-specific design studies utilizing field measurements and computer simulation.

Design based on measurement requires that the vertical stress distribution within pillars be determined and the potential strength for various sized pillars be calculated. It is most useful to measure the vertical stress rise into the pillar under a high loading condition or for the expected "working loads." The stress measurement profiles are used to determine the potential load distributions in pillars of varying dimension and hence to develop a pillar strength relationship suitable for that geological site. An example of stress measurements over a pillar is presented in figure 11; however, the method is limited to determining the potential stress distribution in different pillar widths under the measured loading condition.

Extrapolation of increased loading is more problematic. In weak ground, an approach is to extrapolate the vertical stress buildup from the rib toward the pillar center. This may be possible where the vertical stress buildup approximates a line in the yield zone. This often provides a low estimate of the peak pillar strength and should be considered a working estimate only. An example of this is presented in figure 11*B*. Experience suggests that this is more likely in weak ground; however, in stronger ground the stress buildup is often more exponential and, as such, difficult to extrapolate.

To assess the potential strength under higher loading conditions, a method to redistribute the stress within the pillar associated with an increased average load, or the ability to monitor the effect of additional loading, is required.

Monitoring of stress distributions within pillars during mining can provide elevated loading conditions for analysis. An example is presented in figure 12, whereby small pillars were

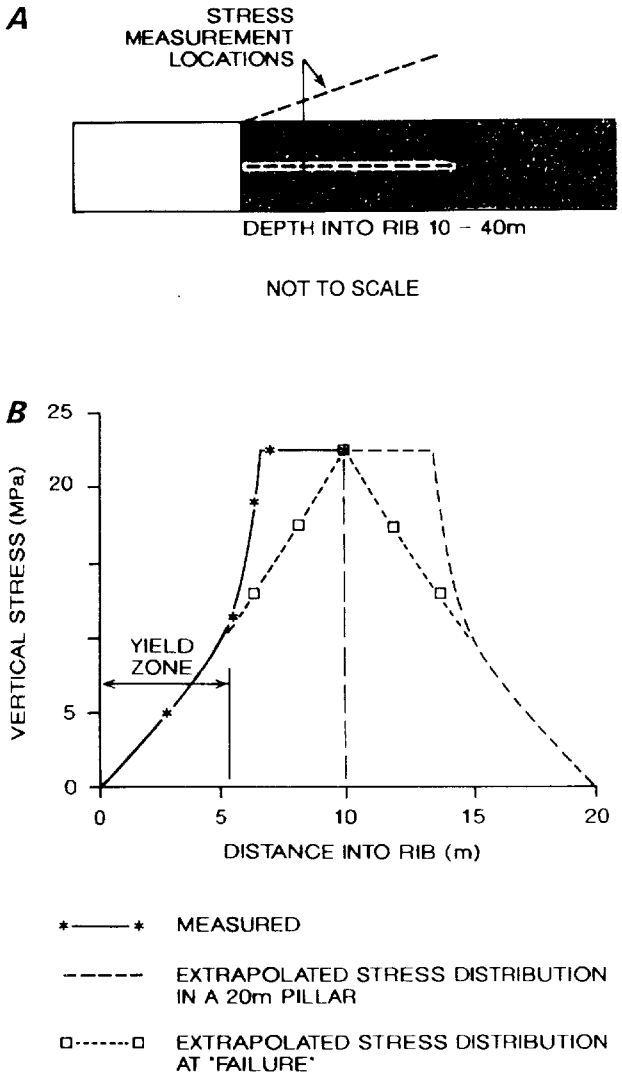

Figure 11.—Stress measurements over ribsides for strength assessment. *A*, typical stress measurement locations; *B*, stress distribution in pillar from measurements.

instrumented with CSIRO HI Cells and monitored until well isolated in the goaf after the passage of a longwall panel.

Computer modeling methods have been developed to simulate the behavior of the strata sections under various stress fields and mining geometries. For mine design, such simulations must be validated against actual ground behavior and stress measurements. This provides confidence that sufficient geological investigation has been undertaken and that the strength properties and deformation mechanisms are being simulated accurately. The computer software developed by Strata Control Technology has been verified in a number of field investigations where computer predictions of stress distributions and rock failure zones have been compared. An example is presented in figure 13, which compares the measured and modeled stress distribution over a yield pillar and solid coal in a deep mine. Another example of computer

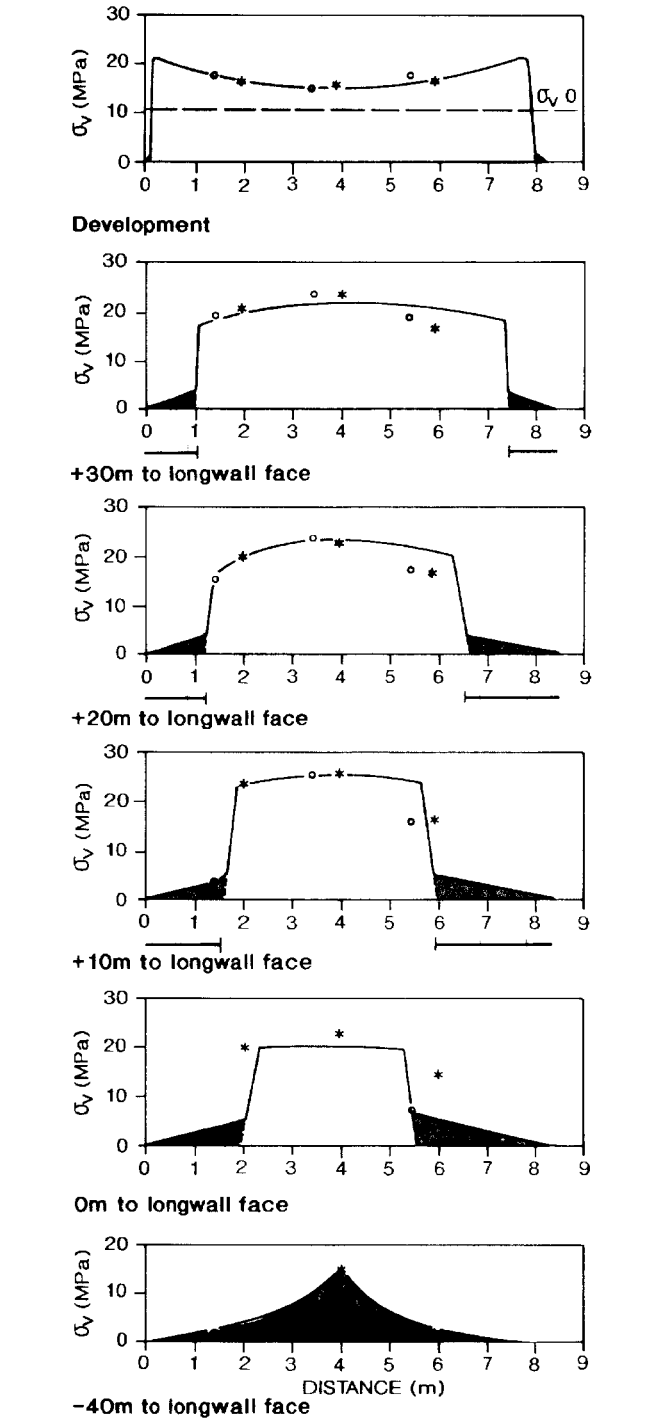

Figure 12.—Example of small pillar monitoring studies indicating pillar stress history.

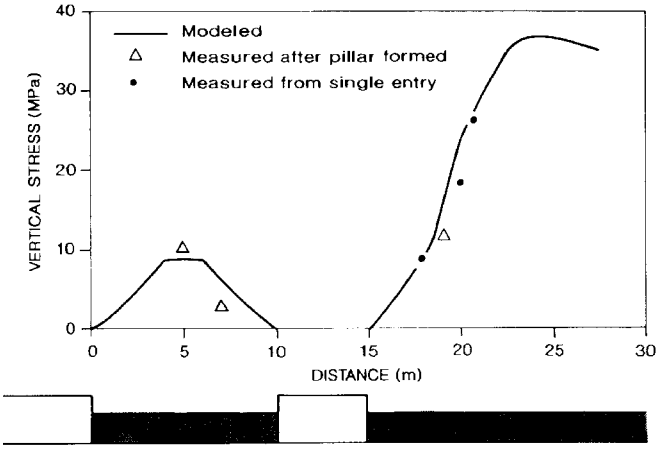

Figure 13.—Stress over yield pillar and adjacent to longwall.

modeling capabilities is presented in figure 14 for weak ground adjacent to a longwall panel. A series of stress measurements was conducted to define the abutment geometry and compared to computer simulations based on the geological section and goaf geometry. The results indicate a very close correlation and that rigorous computer simulation methods can provide a good estimation of the actual stresses and ground failure zones.

One major benefit of computer modeling is that the behavior of roadways adjacent to the pillars can be simulated. In this way, the design of a pillar will reflect not only the stress distribution within it, but also its impact on roadway stability. An example is presented in figure 15 in which the anticipated deformation of a roadway adjacent to a longwall panel under elevated abutment loading was evaluated. The effect of various reinforcement, support, and mining sections was simulated to determine the appropriate mining approach.

In mining situations where there are large areas of solid ground about the working area, the potential for regional collapse of pillars is typically low. Design in these areas usually relates to optimizing roadway conditions and controlling ground movements rather than the nominal pillar strength. Yield pillars and chain pillars are obvious examples of this application. Design must assess the geometry of other pillars

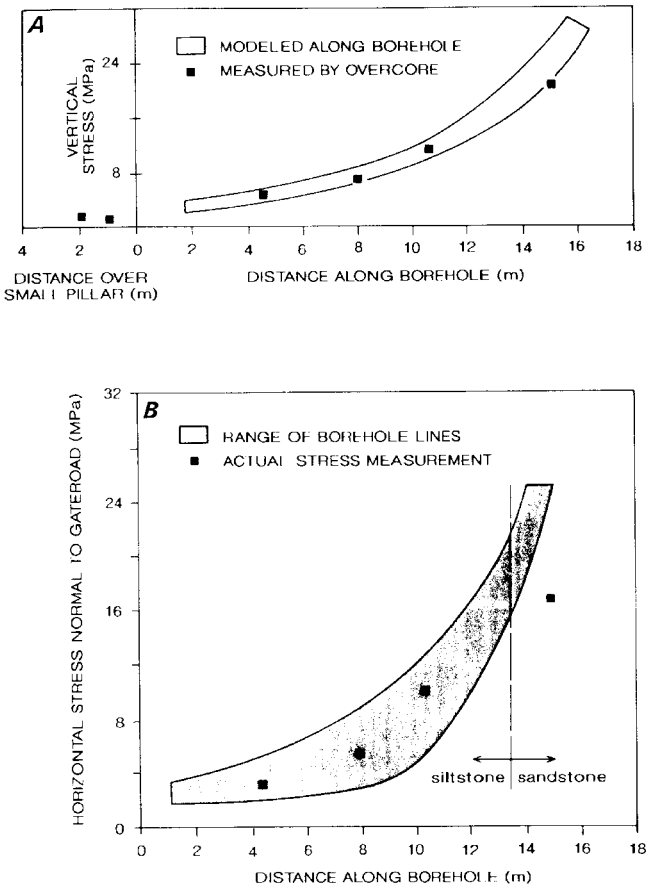

Figure 14.—Comparison of modeled and measured (*A*) vertical and (*B*) horizontal stress over a longwall side abutment. Stress measurements were made in a borehole drilled from an adjacent roadway.

and virgin coal areas in determining the impact of a particular stress distribution within a pillar and the ability of the overburden to span over a yielded pillar and safely redistribute the excess stress to adjacent ground. Figure 13 shows an example of this process for a failed ("yield") pillar adjacent to solid ground.

CHAIN PILLAR DESIGN ISSUES

It has become increasingly apparent from field monitoring and computer simulations of longwall caving that the design of chain pillars requires a larger scale review of ground behavior rather than "small-scale" pillar strength criteria. Microseismic monitoring [Kelly et al. 1998] has demonstrated significant rock fracture above and below chain pillars. Computer modeling of caving [Gale 1998] has also demonstrated rock fracture above and below pillars. Rock failure above and below chain pillars occurs as a result of gross scale stress changes and fluid pressure redistributions.

The strength and loading conditions of chain pillars can reflect the larger scale fracture geometries that may develop. An example of an abutment stress within a pillar at shallow depth (250 m) is presented in figure 16. In this case, rock failure extends over the ribside and shifts the abutment distribution within the pillar.

Modification of the vertical abutment stress distribution has been noted in field monitoring and computer simulations under conditions of high lateral stress. It has been found that the abutment distribution tends to have a lower peak stress, but it spreads over a longer lateral extent. An example is presented in figure 17.

In both of these examples, computer modeling of the caving process within the geological section closely correlates

with the measured data. The use of generalized empirical methods to determine the abutment profile is also presented and indicates that their application is best utilized as initial estimates to be reassessed by site-specific investigations for key design areas.

Rock failure above and below chain pillars does not necessarily occur at all sites; however, experience suggests that this is common. The gross scale rock failure about longwall panels, therefore, requires design for ground control issues rather than pillar design, as traditionally conceived. Field measurement, computer modeling, and microseismic investigations play a key role in defining the design criteria. Empirical databases are also useful; however, the user should be aware of the ground deformation mechanics in order to assess the applicability of the data being used relative to the site conditions to which it would be applied.

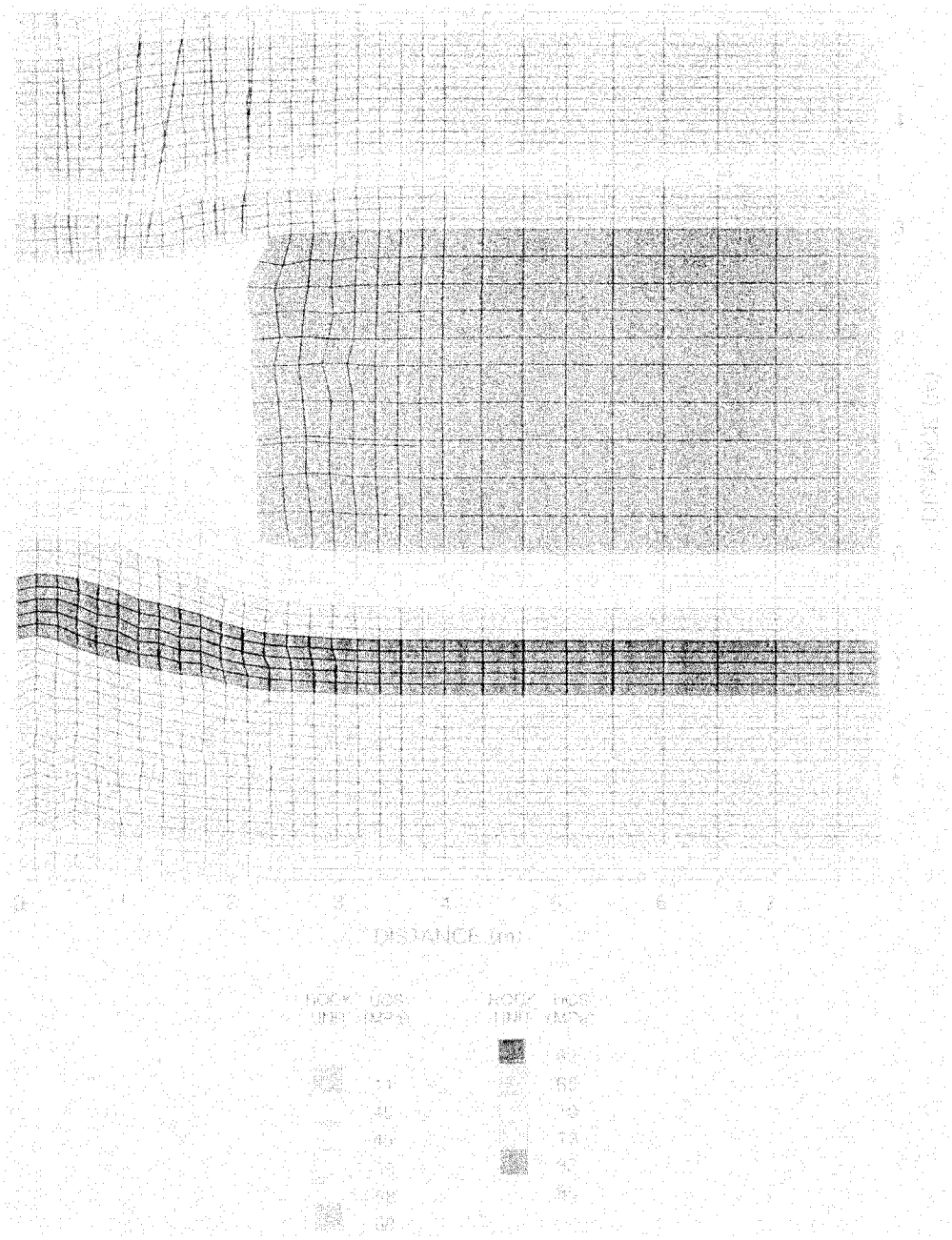

Figure 15.—Simulation of roadway conditions under abutment stress.

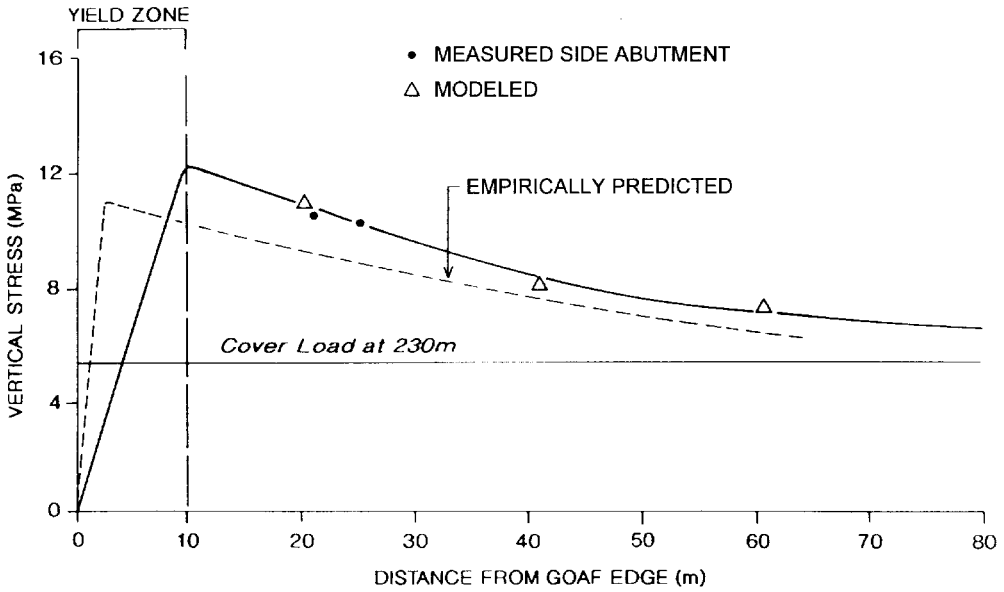

Figure 16.—Longwall side abutment profiles for modeled, measured, and empirical approaches. In this example, rock failure occurred about the pillar, forming a more extensive yield zone.

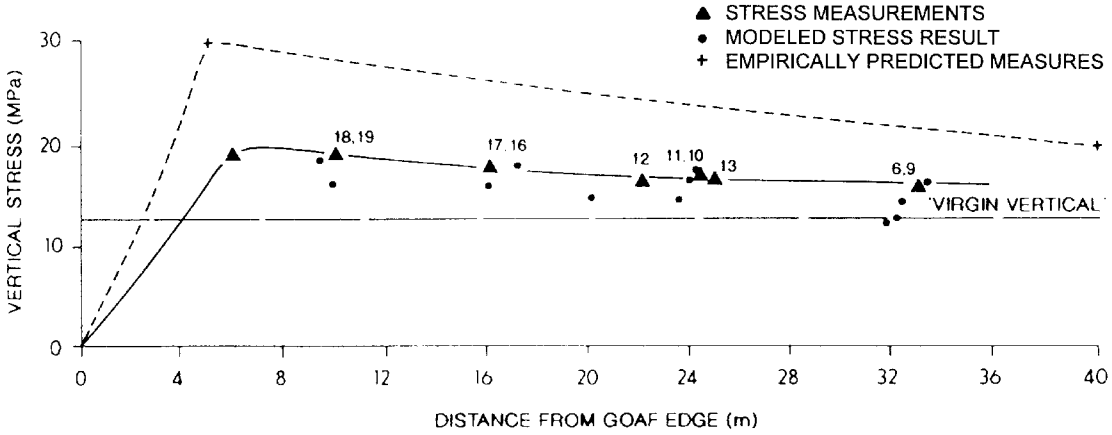

Figure 17.—Longwall side abutment profiles for modeled, measured, and empirical approaches in a high stress mining area.

CONCLUSIONS

The strength characteristics of pillars depend on the strength properties of the strata surrounding the coal.

It is important to consider the postfailure strength of pillars in design, particularly in areas of weak strata where a post-failure strength loss in moderate to large width/height pillars is possible.

Computer simulation methods in association with site measurements are recommended for the design of key layouts that require an assessment of geological variations, pillar size, and stress field changes to optimize the mining operation. This approach also assesses the expected roadway conditions or pillar response for various mine layouts; these can be monitored to determine if the ground is behaving as expected.

Design of pillars adjacent to large extraction areas needs to include the large-scale fracture distributions and, in general, needs to be based on a ground control criterion rather than on a pillar strength criterion only.

REFERENCES

Gale WJ [1996]. Geological issues relating to coal pillar design. In: McNally GH, Ward CR, eds. Symposium of Geology in Longwall Mining, pp. 185-191.

Gale WJ [1998]. Experience in computer simulation of caving, rock fracture and fluid flow in longwall panels. In: Proceedings of the International Conference on Geomechanics/Ground Control Mining and Underground Construction, pp. 997-1007.

Hustrulid WA [1976]. A review of coal strength formulas. Rock Mech *8*:43-50.

Kelly M, Gale WJ, Luo X, Hatherly P, Balusu R, LeBlanc Smith G [1998]. Longwall caving process in different geological environments; better understanding through the combination of modern assessment methods. In: Proceedings of the International Conference on Geomechanics/Ground Control Mining and Underground Construction, pp. 573-589.

Maleki H [1992]. In situ pillar strength and failure mechanisms for U.S. coal seams. In: Proceedings of the Workshop on Coal Pillar Mechanics and Design. Pittsburgh, PA: U.S. Department of the Interior, Bureau of Mines, IC 9315, pp. 73-77.

Mark C, Iannacchione AT [1992]. Coal pillar mechanics: theoretical models and field measurements compared. In: Proceedings of the Workshop on Coal Pillar Mechanics and Design. Pittsburgh, PA: U.S. Department of the Interior, Bureau of Mines, IC 9315, pp. 78-93.

Mark C, Listak JM, Bieniawski ZT [1988]. Yielding coal pillars: field measurements and analysis of design methods. In: Proceedings of the 29th U.S. Symposium on Rock Mechanics. New York, NY: American Institute of Mining, Metallurgical, and Petroleum Engineers, pp. 261-270.

Salamon MDG, Munro AH [1967]. A study of the strength of coal pillars. J S Afr Inst Min Metall, pp. 55-67.

Wilson AH [1972]. An hypothesis concerning pillar stability. Min Eng (London) *131*(141):409-417.

UNIVERSITY OF NEW SOUTH WALES COAL PILLAR STRENGTH DETERMINATIONS FOR AUSTRALIAN AND SOUTH AFRICAN MINING CONDITIONS

By Jim M. Galvin, Ph.D.,[1] Bruce K. Hebblewhite, Ph.D.,[2] and Miklos D. G. Salamon, Ph.D.[3]

ABSTRACT

A series of mine design accidents in the late 1980s resulted in a major research program at the University of New South Wales, Australia, aimed at developing pillar and mine design guidelines. A database of both failed and unfailed Australian underground coal mine pillar case studies was compiled. A procedure was developed to enable the effective width of rectangular pillars to be taken into account. The database was analyzed statistically using the maximum likelihood method, both independently and as a combined data set with the more extensive South African database. Probabilities of failure were correlated to factors of safety. It was found that there was less than a 4% variance in pillar design extraction ratios resulting from each of these approaches. There is a remarkable consistency between the design formulas developed from back-analysis of the two separate national pillar databases containing many different coal seams and geological environments.

[1]Professor and Head, School of Mining Engineering, University of New South Wales, Sydney, Australia.
[2]Professor, School of Mining Engineering, University of New South Wales, Sydney, Australia.
[3]Distinguished professor, School of Mining Engineering, Colorado School of Mines, Golden, CO.

INTRODUCTION

In the 3-year period to 1992, 60 continuous miners were trapped by falls of strata for more than 7 hr in collieries in New South Wales, Australia. In the preceding 2 years, eight coal miners were killed in pillar extraction operations in New South Wales. In the New South Wales and Queensland coalfields, at least 15 extensive collapses of bord-and-pillar workings occurred unexpectedly in the 15-year period to 1992. Six of these collapses occurred in working panels; fortuitously, five occurred during shutdown periods and the sixth occurred while the continuous miner was being flitted to the surface for repairs.

One contributor to these events was the lack of a comprehensive pillar design procedure. Legislation in New South Wales at the time simply required coal pillars to have a minimum width of one-tenth depth or 10 m, whichever was greater. The influence of pillar height on strength received no recognition.

This set of circumstances led to funding by the New South Wales Joint Coal Board of a major research project on pillar design and behavior. The research was undertaken by the School of Mining Engineering at the University of New South Wales (UNSW). The primary objectives of the research were to improve the understanding of coal pillars and associated floor and roof strata behavior under various loading conditions and to incorporate these outcomes into the mine design knowledge base.

RESEARCH METHODOLOGY

The approach adopted to pillar design was based on that developed for square pillars by Salamon and Munro [1966, 1967]. However, the extensive use of rectangular and diamond-shaped pillars in Australia required more detailed consideration of the *effective width* of parallelepiped pillars and the effect of this width on pillar strength.

Firstly, an adequate Australian database of failed and unfailed pillar case histories was established. A relationship was then developed to factor in the influence of rectangular and diamond-shaped pillars, which comprised just over 50% of the database. This database was then subjected to rigorous statistical analysis using a range of techniques in order to quantify parameters associated with each of two generally accepted empirical formulas for describing pillar strength. This facilitated the establishment of correlation, for all strength expressions, between the probability that a formula would yield a successful design versus the respective design factor of safety.

The Australian database was also combined with the much larger and long-established South African database, and the analysis was repeated to determine if the two population bases could be considered as one. A close correlation was obtained, leading to an increased level of confidence in this methodology and to a number of more universal conclusions concerning pillar design.

EMPIRICAL COAL PILLAR STRENGTH ESTIMATIONS

The development of computer and numerical technologies in recent decades has facilitated, at least in principle, the analysis of stresses in pillars and their foundations, i.e., the roof and floor strata. Unfortunately, physical experimentation has not advanced equally rapidly. Hence, the understanding of the intrinsic constitutive laws controlling the behavior of yielding rocks is still unsatisfactory. More immediate problems include the significant discrepancies between the physical properties exhibited by rocks in situ and those measured in the laboratory by testing small specimens. These problems relate to the effects of size and shape on rock strength.

Many investigators have proposed simple empirical formulas to describe the strength of coal pillars. The most common feature of most of these empirical relationships is that they define strength ostensively only in terms of the linear dimensions of the pillars and a multiplying constant, representing the strength of the unit volume of coal. Investigators over the years have proposed formulas that belong to one of two types. One type defines pillar strength simply as a linear function of the width-to-height (w/h) ratio:

$$F_{s1} = K_1 \left[r \% (1 - r) \frac{w}{h} \right], \qquad (1)$$

where K_1 is the compressive strength of a cube and r is a dimensionless constant. The quantities of w and h are the width and height of the pillar, respectively.

If the notation

$$R = w/h \qquad (2)$$

is introduced, then equation 1 becomes

$$F_{s1} = K_1[r + (1 - r)R]. \quad (3)$$

According to this formula, geometrically similar pillars have the same strength regardless of their actual dimensions.

A second commonly used pillar strength formula takes the form

$$F_{s2} = K_2\left(\frac{w}{w_0}\right)^{\alpha}\left(\frac{h}{h_0}\right)^{\beta}, \quad (4)$$

which is expressed in a dimensionally correct form. α and β are dimensionless parameters; w and h are the linear dimensions of the pillar. Multiplier K_2 is the strength of a reference body of coal of height h_0 and a square cross section with side length w_0.

In most instances, the reference body is taken to be cube of unit volume for convenience's sake, in which case h_0 and w_0 are both unity and can be omitted from the formula. Expressions belonging to this family are referred to as *power law* strength formulas. In contrast to formulas of the form of equation 1, these formulas are also volume-sensitive.

EFFECTIVE WIDTH OF PARALLELEPIPED PILLARS

The development of statistically based pillar design formulas rests minimally upon the premise that a fairly large and tolerably reliable database of unfailed and failed pillar panels can be compiled. Salamon et al. [1996] have identified a number of strict criteria that must be satisfied before a case can be included in the database. One of these that must be appreciated when applying the outcomes of this pillar design research is that these outcomes apply only to competent roof and floor environments, i.e., the database relates only to failures of the coal pillar element of the pillar system, not to the roof or floor elements.

Against this background, an Australian database of 19 failed and 16 unfailed cases was assembled. Rectangular pillars comprised eight of the failed and nine of the unfailed cases. Diamond-shaped pillars comprised one failed case. In order to preserve in these circumstances the availability of the strength formulas derived for square pillars, many researchers have proposed the introduction of an *effective* width.

One of the most basic approaches is to define the effective width, w_e, as

$$w_e = \sqrt{w_1 w_2}, \quad (5)$$

where w_1 = minimum pillar width (measured along roadway)

and w_2 = maximum pillar width (measured along roadway).

In situations where w_2 is not extremely different to w_1, this approach has merit. However, when $w_2 \gg w_1$, the equation produces an unrealistic effective pillar width (table 1).

Table 1.—Application of various effective pillar width formulas
(Width and height in meters)

w_1	w_2	h	$\sqrt{w_1 w_2}$	$4A_p/C_p$	w1
100	100	3	100.0	100	100
80	100	3	89.4	88.9	88.9
50	100	3	70.7	66.7	66.7
30	100	3	54.7	46.2	46.2
20	100	3	44.7	33.3	33.3
15	100	3	38.7	26.1	21.7
10	100	3	31.6	18.2	10.7
1	100	3	10.0	2.0	1

The most promising recommendation has come from Wagner [1974, 1980], who, making use of the concept of hydraulic radius, suggested that the effective width be defined as

$$w_e = 4\frac{A_p}{C_p}, \quad (6)$$

where A_p and C_p are the cross-sectional area and the circumference of the pillar, respectively.

Application of equation 6 produces effective pillar width similar to that of equation 5 when w_1 is greater than about $0.5w_2$ (table 1). At moderate to low values of w_1 ($0.4w_2 \geq w_1 \geq 0.2w_2$), equation 6 predicts a smaller effective width, which is more sensible from a mechanistic viewpoint. However, at very low values of w_1 ($w_1 < 0.2w_2$), the equation is still considered to overestimate the effective pillar width. This is because when a pillar is narrow, failure is likely to occur across the narrow dimension before sufficient confinement is generated in the longitudinal direction to be of benefit.

This leads to the concept that rectangular and irregular pillars need to be of a critical minimum width before benefit is gained from confinement generated in the longitudinal direction. This benefit can be expected to ramp up to a plateau level as the minimum width increases. Furthermore, it is reasonable to expect that this minimum critical width will be a function of mining height, increasing with increasing mining height.

The need to nominate a minimum critical pillar width has been incorporated into the analysis by modifying equation 6 on the basis that almost all pillars can be regarded as parallelepipeds, i.e., their bases are parallelograms (figure 1). Pillars therefore have side lengths w_1 and w_2 ($w_1 \# w_2$) and an internal angle $2 \# 90°$. Equation 6 then becomes

$$w_{e o} ' 1_o w, \tag{7}$$

where w is the minimum width of the pillar, i.e.,

$$w ' w_1 \sin 2 \tag{8}$$

and the dimensionless factor 1_o is defined by

$$1_o ' \frac{2w_2}{w_1 \% w_2}. \tag{9}$$

The range of this factor is $1 \# 1_o < 2$, which is encountered as the aspect ratio moves from unity toward infinity. Experience indicates that much before the complete failure of a pillar, its edges are already yielding. Thus, if the w/h ratio in one direction of a rectangular pillar is low, one of the principal stresses confining its core will remain small, and this stress, together with the maximum stress, will control failure.

Hence, the extra confinement that may arise from the aspect ratio will have little or no effect. It is suggested that such apprehension may be catered for by postulating that the effective width is the minimum width, i.e., $w_e ' w$ as long as $R < R_l$, and it becomes $w_e ' w_{eo}$ when $R > R_u$.

In the intermediate range, i.e., when $R_l \# R \# R_u$, the effective width changes smoothly in accordance with

$$w_e ' w 1_o^{\frac{R\&R_l}{R_u\&R_l}} ' w 1. \tag{10}$$

Here, the choice of the limiting w/h ratios is open to judgment. It appears reasonable, however, to use the following values:

$$R_l ' 3 \qquad R_u ' 6 \tag{11}$$

Table 1 and figure 2 show the effects of the various approaches when applied to calculating the effective width of a 100-m-long, 3-m-high rectangular pillar.

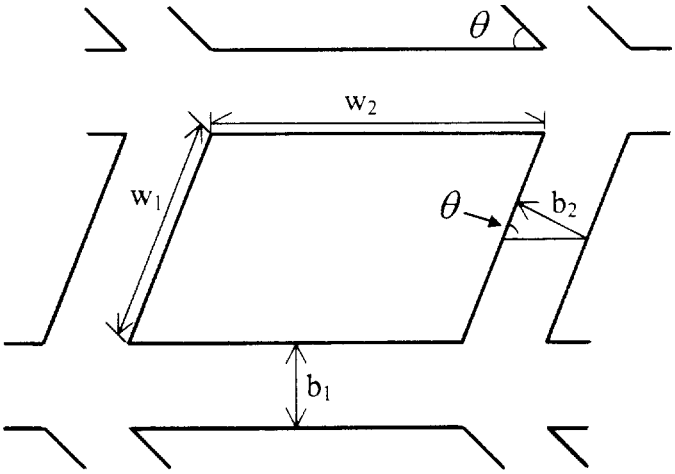

Figure 1.—Definition of mining variables associated with a parallelepiped pillar.

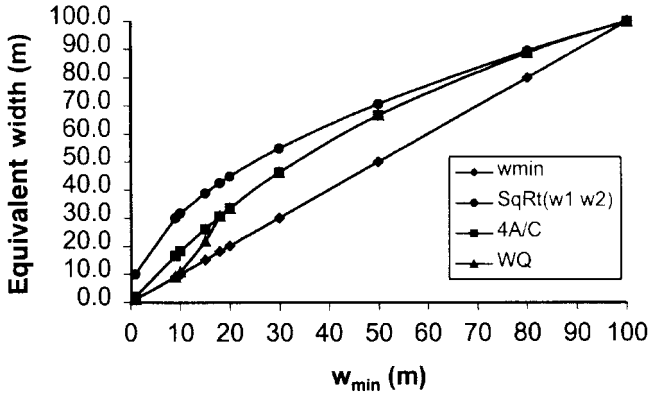

Figure 2.—Comparison of the various proposals for calculating the effective width of a 100-m-long, 3-m-high rectangular pillar.

Using the concept of effective width, the power law in equation 4 can be rewritten for pillars with a general parallelepiped shape:

$$F_{s2} ' K_2 w " h \$ 1 " \tag{12}$$

An alternative form of this formula expresses the strength as the function of the pillar volume V and the w/h ratio R:

$$F_{s2} ' K_2 V^a R^b 1 ", \tag{13}$$

where the volume refers to a dummy square pillar of width w and height h, and the w/h ratio is calculated from the minimum pillar width:

$$V ' w^2 h \qquad R ' \frac{w_1 \sin 2}{h} ' \frac{w}{h} \tag{14}$$

The new constants a and b can be defined in terms of constants " and $:

$$a = \frac{1}{3}(\alpha + \beta) \qquad b = \frac{1}{3}(\alpha - 2\beta) \tag{15}$$

Experience has shown that the original power law formula (equation 4) tends to underestimate the strength of squat pillars, i.e., pillars with a w/h ratio in excess of about 5. To cater for this problem, Salamon and Wagner [1985] suggested an extension of equation 4 into the range of higher w/h ratios. This extension, after adaptation to pillars of parallelepiped shape, is

$$F_{s2} = K_2 V^a R_o^b \lambda^{\alpha} \left\{ \frac{b}{\gamma} \left[\left(\frac{R}{R_o} \right)^{\gamma} - 1 \right] + 1 \right\}, \tag{16}$$

which is valid if $R > R_o$ and where λ is defined in equation 10. This particular form was chosen to ensure that there is a smooth transition between this and equation 13 at $R = R_o$ [Salamon and Wagner 1985]. Here, R_o and γ are appropriately chosen constants. The expression is often referred to as the *squat pillar strength* formula. Since its inception, it has been applied widely in the Republic of South Africa using the following pair of constants:

$$R_o = 5 \qquad \gamma = 2.5 \tag{17}$$

In critical situations, the judgment exercised in deriving the effective pillar width relationship may be regarded as too speculative. This concern can be addressed by either choosing an elevated design factor of safety to account for this level of uncertainty or reverting to the use of the minimum pillar width in pillar strength calculations.

Another aspect to the use of rectangular pillars is the calculation of pillar load. In calculating the tributary load, the true dimensions need to be employed. Thus, the pillar load assumes the following form:

$$q_m = \gamma H \alpha \frac{(w + b_1)(w_2 + b_2 / \sin\theta)}{w w_2} \tag{18}$$

In this relationship, α is a modifier. It is unity in all cases where the pillar burden is the conventional tributary load. If, however, due to secondary extraction the pillar load is believed to differ from this value, the load can be adjusted by applying this factor. Moreover, to remain consistent with earlier calculations, γ is taken to be: $\gamma = 1.1$ psi/ft $= 24.8827$ kN/m^3 $= 24.8827$ kPa/m.

UNSW INITIAL DESIGN FORMULAS

In 1992, following a number of serious incidents related to the lack of restriction on pillar height, the Chief Inspector of Coal Mines in New South Wales required operators to obtain approval to mine at heights exceeding 4 m. To address the need for a pillar design methodology, the UNSW research team undertook in 1995 a preliminary analysis of its database [Hocking et al. 1995]. At the time, the database comprised 14 collapsed cases and 16 stable cases that satisfied the selection criteria. The database was analyzed statistically using the full maximum likelihood method. Galvin and Hebblewhite [1995] subsequently published the following pillar design formulas, which find current application in Australia:

$$F_{s2} = 7.4 \frac{w^{0.46}}{h^{0.66}} \quad \text{(MPa)} \tag{19a}$$

and its squat pillar version (R > 5):

$$F_{s2} = \frac{19.24}{w^{0.133} h^{0.067}} \left\{ 0.237 \left[\left(\frac{w}{5h} \right)^{2.5} - 1 \right] + 1 \right\} \quad \text{(MPa)} \tag{19b}$$

A conservative approach was adopted, and the minimum pillar width was proposed as the effective width. It follows, therefore, that $\lambda = 1$ in these expressions. There was little difference in the pillar strength obtained by allowing all parameters to float in the statistical analysis as opposed to allowing only the K values to float and fixing the other parameters to be the same as those used for many years in the Republic of South Africa. To avoid confusion and to facilitate the introduction of the formulas, therefore, only those formulas derived by allowing the K values to float were presented to operators. The formula for strength based on the linear relationship took the following form:

$$F_{s1} = 5.36(0.64 + 0.36R) \quad \text{(MPa)} \tag{20}$$

UNSW REFINED (RECTANGULAR) FORMULAS

In 1996, a more comprehensive statistical analysis of the expanded Australian database was completed that incorporated the effective width of rectangular pillars as defined earlier [Salamon et al. 1996]. Statistical methods included least squares, limited maximum likelihood, and full maximum likelihood. Both power law models and linear law models were evaluated, and all parameters were allowed to float. In all instances, the power law model gave better correlations.

The following strength formulas were found to best describe the observed behavior of pillars in New South Wales and Queensland:

$$F_{s2} = 8.60 \frac{(w1)^{0.51}}{h^{0.84}} \quad \text{(MPa)} \qquad (21a)$$

The corresponding expression for squat pillars is given by

$$F_{s2} = \frac{27.63\,1^{0.51}}{w^{0.220}\,h^{0.110}} \left\{ 0.290 \left[\left(\frac{w}{5h} \right)^{2.5} - 1 \right] + 1 \right\} \quad \text{(MPa)} \qquad (21b)$$

In these expressions, $w = w_1 \sin 2$, and the effective width factor 1 is as defined in equation 10.

The relationship between pillar strength and pillar load produced by these equations for each point in the database is shown in figure 3. Design factors of safety associated with the probability of achieving a stable design are shown in table 2.

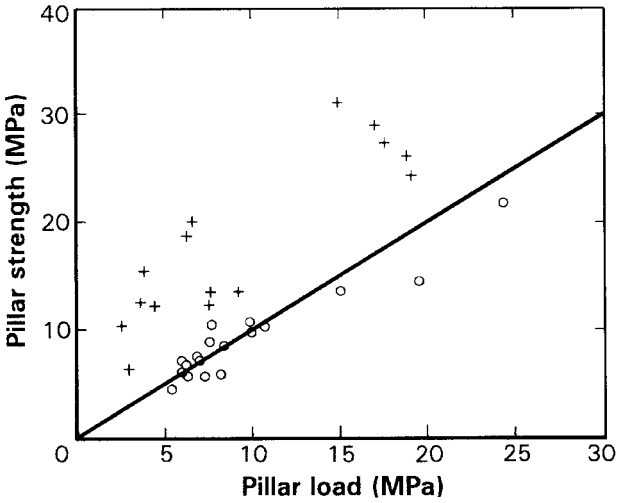

Figure 3.—Pillar strength and pillar load relationship for both the failed (o) and unfailed (+) Australian cases.

Table 2.—Probability of failure versus factor of safety

Probability of failure	Factor of safety
8 in 10	0.87
5 in 10	1.00
1 in 10	1.22
5 in 100	1.30
2 in 100	1.38
1 in 100	1.44
1 in 1,000	1.63
1 in 10,000	1.79
1 in 100,000	1.95
1 in 1,000,000	2.11

REANALYSIS OF THE SOUTH AFRICAN DATABASE

The original extensive South African coal pillar database used by Salamon and Munro in 1966 has since been updated and supplemented by Madden and Hardman [1992]. This combined South African database comprises 44 failed and 98 unfailed cases. It has also been reanalyzed using the same statistical techniques used for the Australian database. Two failed cases were later omitted from the data set [Salamon et al. 1996].

This analysis has produced the following strength formulas:

$$F_{s2} = 6.88 \frac{(w1)^{0.42}}{h^{0.60}} \quad \text{(MPa)} \qquad (22a)$$

The corresponding expression for squat pillars (R > 5) is given by

$$F_{s2} = \frac{16.36\,1^{0.42}}{w^{0.116}\,h^{0.058}} \left\{ 0.215 \left[\left(\frac{w}{5h} \right)^{2.5} - 1 \right] + 1 \right\} \quad \text{(MPa)} \qquad (22b)$$

The linear version of the strength estimator is simply

$$F_{s1} = 5.60(0.69 + 0.31R) \quad \text{(MPa)} \qquad (23)$$

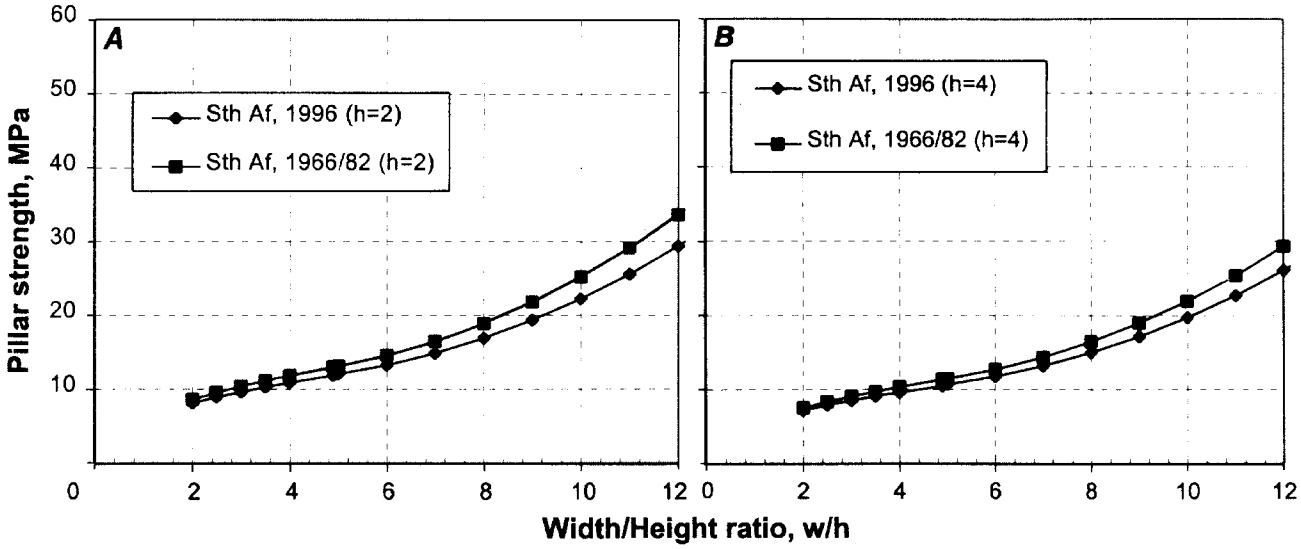

Figure 4.—Comparison between South African power formulas, 1966/82 and 1996. *A*, h ' 2 m; *B*, h ' 4 m.

Figure 4 shows the comparison between the pillar strength produced by equations 22a and 22b and that predicted by the original Salamon and Munro formula and its modified squat pillar form. In the case of a mining height of 2 m, the figure shows that for a given pillar strength, pillars designed with the updated formulas may need to be about 2 m wider. For a bord width of 6 m at a w/h ratio of 10, this results in about 3% less resource recovery. For similar circumstances in a 4-m mining height, the increase in pillar size is on the order of 3.2 m.

COMBINED AUSTRALIAN AND SOUTH AFRICAN DATABASES

A further step in the research program was to combine the South African and Australian databases and to analyze them as a combined population, then compare and contrast them with the two independent data populations for each country. This combined database comprised 177 cases of pillar systems, including 61 collapsed cases. This produced the following formulas:

$$F_{s2} = 6.88 \frac{\sqrt{w1}}{h^{0.7}} \quad \text{(MPa)} \qquad (24a)$$

For R > 5, the squat version of this expression takes the following form:

$$F_{s2} = \frac{19.05\sqrt{1}}{w^{0.133} h^{0.066}} \left\{ 0.253 \left[\left(\frac{w}{5h} \right)^{2.5} \& 1 \right] \%1 \right\} \quad \text{(MPa)} \qquad (24b)$$

The corresponding linear formula is simply

$$F_{s1} = 5.41(0.63 \% 0.37R) \quad \text{(MPa)} \qquad (25)$$

Figure 5 shows failed and unfailed cases in the load plane. The figure illustrates a fairly good discrimination between the two sets of points. Only one unfailed point occurs on the wrong side of the s ' 1 line, and the median failed cases is 1.039.

Figure 6 shows a comparison between pillar strengths using power law estimators derived from the Australian, South African, and combined Australian-South African databases. The closeness of the predictions is remarkable considering the geographical separation of the Australian and South African coalfields.

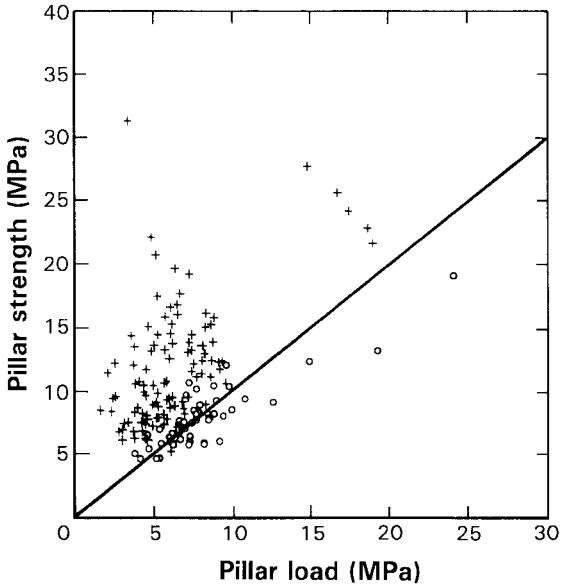

Figure 5.—The failed (o) and unfailed (+) cases in a pillar strength versus pillar load plot using the combined Australian-South African database.

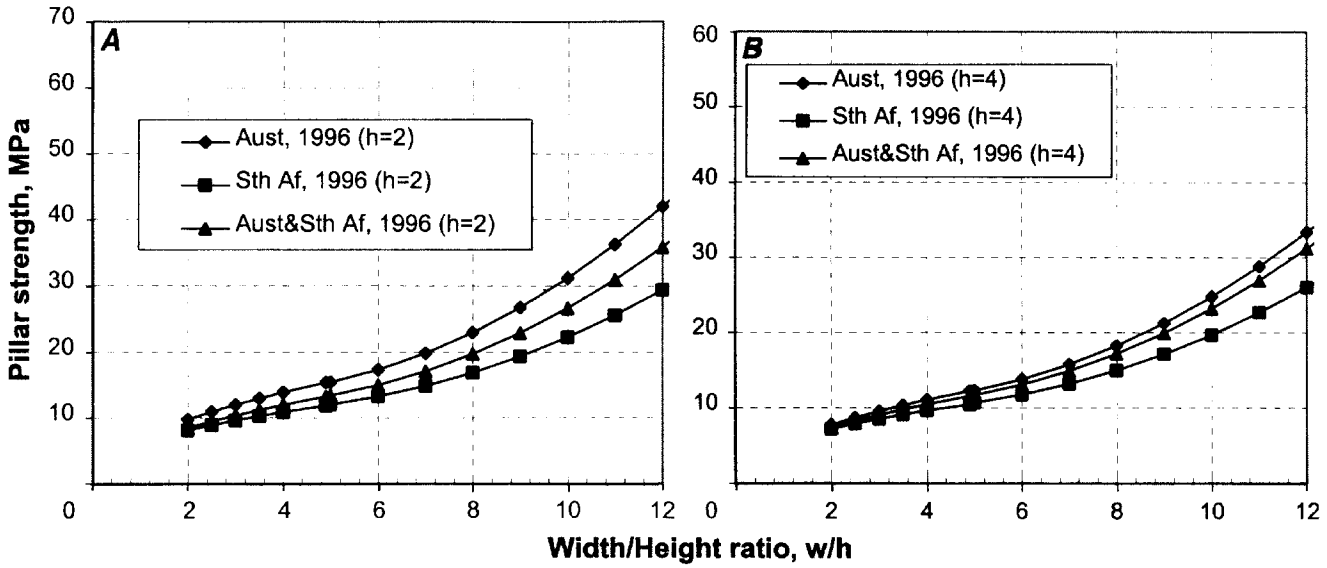

Figure 6.—Comparison between power law strength formulas derived for the Australian, South African, and combined databases. *A*, h ' 2 m; *B*, h ' 4 m.

CONCLUSIONS

The statistical analysis of the Australian database indicates that the method proposed for calculating the effective width of parallelepiped pillars produced sensible outcomes. However, it must be remembered that, although of sufficient size to be statistically significant, the parallelepiped database is small. The method should therefore be used with caution.

In order to enhance confidence in the pillar design procedure, including the use of the effective pillar width method, additional research was undertaken. It was noted that the formula derived from the initial Australian database closely resembled the original Salamon-Munro expression. This somewhat surprising resemblance prompted further research and enlargement of the database. The larger database yielded pillar strengths that again were similar to those obtained from the initial UNSW research and by Salamon and Munro. The combination of the Australian and South African databases reinforced the original impression, namely, that the underlying pillar strengths in these countries resembled each other closely.

The outcome of the investigation lends support to the view expressed by Mark and Barton [1996]. They suggested that strength values obtained in the laboratory cannot be utilized in a meaningful way in pillar design and that the variation in the strength of pillars of the same size can be disregarded in many instances. Mark and Barton [1996] emphasize that they do not claim that the in situ strength of all U.S. coal is the same. Their study merely showed that a uniform strength is a better approximation than one based on laboratory testing. Although the UNSW research conclusions are encouraging, complacency is not justified. The formulas are based on competent roof and floor conditions. Significantly different pillar strengths may be associated with abnormal strata behavior mechanisms. Because pillars with w/h ratios greater than 10 have not been tested to destruction, it must also be recognized that neither linear nor power law formulas have been validated at w/h ratios greater than about 8.

It cannot be overemphasized that, because the design formulas have been developed on a probabilistic basis, they need to be reviewed periodically as the database expands and the understanding of pillar mechanics advances. A fundamental rule of empirical research is that the results should be used within the range of data used in their derivation. Extrapolation with empirical formulas is always fraught with danger.

REFERENCES

Galvin JM, Hebblewhite BK [1995]. UNSW pillar design methodology. Sydney, Australia: University of New South Wales, School of Mining Engineering, Research Release No. 1.

Hocking G, Anderson I, Salamon MDG [1995]. Coal pillar strength formulae and stability criteria. Sydney, Australia: University of New South Wales, School of Mining Engineering, Research Report 1/95.

Madden BJ, Hardman DR [1992]. Long-term stability of bord-and-pillar workings. In: Proceedings of the Symposium on Construction Over Mined Areas. Pretoria, Republic of South Africa.

Mark C, Barton TM [1996]. The uniaxial compressive strength of coal: should it be used to design pillars? In: Ozdemir L, Hanna K, Haramy KY, Peng S, eds. Proceedings of the 15th International Conference on Ground Control in Mining. Golden, CO: Colorado School of Mines, pp. 61-78.

Salamon MDG, Munro AH [1966]. A study of the strength of coal pillars. Transvaal and Orange Free State Chamber of Mines, Research Report No. 71/66.

Salamon MDG, Munro AH [1967]. A study of the strength of coal pillars. J S Afr Inst Min Metall, pp. 55-67.

Salamon MDG, Wagner H [1985]. Practical experiences in the design of coal pillars. In: Green AR, ed. Proceedings of the 21st International Conference of Safety in Mines Research Institutes (Sydney, Australia). Balkema, pp. 3-9.

Salamon MDG, Galvin JM, Hocking G, Anderson I [1996]. Coal pillar strength from back calculation. Sydney, Australia: University of New South Wales, School of Mining Engineering, Research Report 1/96.

Wagner H [1974]. Determination of the complete load deformation characteristics of coal pillars. In: Proceedings of the Third International Congress on Rock Mechanics. International Society for Rock Mechanics, pp. 1076-81.

Wagner H [1980]. Pillar design in coal mines. J S Afr Inst Min Metall, pp. 37-45.

PRACTICAL BOUNDARY-ELEMENT MODELING FOR MINE PLANNING

By Keith A. Heasley, Ph.D.,[1] and Gregory J. Chekan[2]

ABSTRACT

As part of the initial investigation and validation of a new boundary-element formulation for stress modeling in coal mines, the underground stresses and displacements at two multiple-seam coal mines with unique stress problems were modeled and predicted. The new program, LAMODEL, calculates stresses and displacements at the seam level and at requested locations in the overburden or at the surface. Both linear elastic and nonlinear seam materials can be used, and surface effects, multiple seams, and multiple mining steps can be simulated. In order to most efficiently use LAMODEL for accurate stress prediction, the program is first calibrated to the site-specific geomechanics based on previously observed stress conditions at the mine. For this calibration process, a previously mined area is "stress mapped" by quantifying the observed pillar and strata behavior using a numerical rating system. Then, the site-specific mechanical properties in the model are adjusted to provide the best correlation between the predicted stresses and the observed underground stress rating. Once calibrated, the model is then used to predict future stress problems ahead of mining. At the two case study mines, the calibrated models showed good correlation with the observed stresses and also accurately predicted upcoming high stress areas for preventive action by the mines.

[1]Supervisory physical scientist.
[2]Mining engineer.
Pittsburgh Research Laboratory, National Institute for Occupational Safety and Health, Pittsburgh, PA.

INTRODUCTION

Mine planners have a variety of modeling methods, both empirical and numerical, for analyzing pillar stresses and determining safe pillar sizes for various mine geometries and geologic structures. Empirical methods emphasize the collection and interpretation of case histories of pillar performance. The Analysis of Longwall Pillar Stability (ALPS) and Analysis of Retreat Mining Pillar Stability (ARMPS) programs are two such empirical programs that are derived from large databases of real-world pillar studies and can be used for determining pillar sizes for single-seam longwall and retreat room-and-pillar mining, respectively [Mark 1992; Mark and Chase 1997]. The Virginia Polytechnic Institute and State University, Blacksburg, VA, recently developed a comparable empirical program called Multi-Seam Analysis Package (MSAP) for sizing pillars for multiple-seam situations [Kanniganti 1993]. These empirical programs are closely linked to reality and very user-friendly; for many typical mining geometries, they work extremely well.

However, it is difficult to apply these empirical programs to mining situations beyond the scope of the original empirical database. Therefore, when complicated stress conditions arise from complex single- or multiple-seam mining geometries, numerical modeling techniques such as finite-element, boundary-element, discrete-element, or finite-difference are usually applied. In general, these numerical, or analytical, design methods are derived from the fundamental laws of force, stress, and elasticity. Their primary advantage is that they are very flexible and can quickly analyze the effect of numerous geometric and geologic variables on mine design. Their primary disadvantage is that they require difficult-to-obtain and/or controversial information about material properties, failure criteria, and postfailure mechanics. In this paper, the solid foundation of empirical pillar design and in-mine observation is combined with the flexibility of numerical modeling to provide a practical technique for mine planning in difficult situations.

LAMODEL

In order to analyze the displacements and stresses associated with the extraction of large tabular deposits such as coal, potash, and other thin vein-type deposits, the displacement-discontinuity variation of the boundary-element technique is frequently the method of choice. In the displacement-discontinuity approach, the mining horizon is treated mathematically as a discontinuity in the displacement of the surrounding media. Using this technique, only the planar area of the seam needs to be discretized, or gridded, in order to obtain the stress and displacement solution on the seam. Often, this limited analysis is sufficient, because in many applications only the distributions of stress and convergence on the seam horizon are of interest. Also, by limiting the detailed analysis to only the seam, the displacement-discontinuity method provides considerable computational savings over other techniques that discretize the entire body (such as finite-element, discrete-element, or finite-difference). It is a direct result of this computational efficiency that the displacement-discontinuity method is able to handle large areas of tabular excavations, which is needed in many practical coal mining problems.

A displacement-discontinuity program incorporating a laminated medium was recently developed by the National Institute for Occupational Safety and Health, Pittsburgh Research Laboratory; this new program is called LAMODEL. Traditional displacement-discontinuity programs use a homogeneous isotropic elastic formulation that simulates the overburden as one solid material. In contrast, the LAMODEL program simulates the geologic overburden stratifications as a stack of layers with frictionless interfaces. Specifically, each layer is homogeneous isotropic elastic and has the same elastic modulus, Poisson's ratio, and thickness. This "homogeneous layering" formulation does not require specifying the material properties for each individual layer, yet it still provides a realistic suppleness to the mining overburden that is not possible with the classic homogeneous isotropic elastic overburden model. From our experience, this suppleness provides a more accurate strata response for modeling local deformations, interseam interactions, and/or surface subsidence. The LAMODEL program calculates stresses and displacements at the seam level and at requested locations in the overburden or at the surface. Both linear elastic and nonlinear seam materials can be used. The program also has the ability to analyze (1) the interseam stresses resulting from multiple-seam mining, (2) the effects of topographic relief on pillar stress and gob loading, (3) the stress changes during mining through multiple mining steps, and (4) the surface subsidence.

INITIAL MATERIAL PROPERTY GENERATION

As mentioned earlier, one of the most difficult aspects of using a numerical model is determining the correct (most accurate) material properties for input. After developing numerous displacement-discontinuity models and then comparing their results with field measurements and observations, a fairly streamlined, systematic technique for developing initial material properties was developed. Initially, the critical material properties (coal, gob, and rock mass) are

determined using a combination of laboratory research, empirical formulas, and experience. Then, in the calibration process, these initial material properties are systematically adjusted in subsequent runs of the model until the results correspond as closely as possible to field observations. This technique for determining material properties has many similarities to the procedure used by Karabin and Evanto [1999].

First, to address the problem of determining the input coal behavior, the basic coal strengths are derived from the empirical pillar strength formulas, which are solidly based on observed pillar behavior. Specifically, the peak strength of a model coal element is directly determined based on an in situ coal strength and its distance from the edge of the pillar [Heasley 1998] using the stress gradient implied by the Bieniawski pillar strength formula [Mark and Chase 1997]. This peak strength is then implemented using an elastic, perfectly plastic material model [Zipf 1992]. For an initial estimate, an in situ coal strength of 6.2 MPa (900 psi) [Mark and Barton 1997] and an elastic modulus of 2 GPa (300,000 psi) is typically used.

This general procedure for generating the initial coal properties for elements in LAMODEL fulfills a number of practical requirements. It provides LAMODEL pillars with peak strengths that closely follow the empirically proven Mark-Bieniawski pillar strength formula and with stress profiles that closely follow the Bieniawski stress profile. As opposed to a simple elastic material model with no load limit, this procedure using elastic-plastic material allows the pillars to reach a maximum load-carrying capacity and then realistically shed additional load to surrounding areas. Table 1 presents typical elastic-plastic material input values for 3-m (10-ft) coal elements in a 1.8-m (6-ft) seam with a 6.2-MPa (900-psi) in situ coal strength. (Note that the peak stress for the coal elements decreases from the core to the rib of the pillar, which gives the pillar the proper stress profile.)

Second, to address the gob loading and compaction behavior, a combination of laboratory research and modeling experience is used. In the laboratory, Pappas and Mark [1993] found that an exponentially strain-hardening material with a tangent modulus that increases linearly with stress provided a reasonable representation of simulated gob material. This material model is implemented in LAMODEL [Heasley 1998] and is used for the gob modeling. The necessary input for this material is initial modulus, final modulus, and final vertical stress. From experience, these three values are initially set at 6.2 MPa (900 psi), 110 MPa (16,000 psi) and 27.6 MPa (4,000 psi), respectively (see table 1).

Table 1.—Typical elastic-plastic coal and strain-hardening gob parameters

COAL ELEMENTS: UPPER MINE		
Element	Peak stress, MPa	Peak strain
A (core)	85.9	0.04152
B	56.1	0.02712
C	38.3	0.01992
D (rib)	11.4	0.00552
GOB ELEMENTS		
Initial modulus, MPa	Final modulus, MPa	Final stress, MPa
6.2	110	27.6

The third critical set of material inputs in LAMODEL is for the overburden and consists of a lamination thickness and an elastic modulus. In LAMODEL, the lamination thickness has a major influence on the stress and displacement distribution at the seam and throughout the overburden. Prior research [Heasley 1998] comparing LAMODEL results with empirical relationships and measured field data shows that for large-scale stress distributions (such as longwall abutments) lamination thicknesses ranging from 15 to 100 m (50 to 300 ft) provide the best match to field measurements. However, when small-scale stress distributions (such as interseam stresses) or overburden displacements (such as subsidence) are of primary concern, then lamination thicknesses ranging from 3 to 15 m (10 to 50 ft) provide the best match to field observations [Karabin and Evanto 1999; Pappas and Mark 1993]. A lamination thickness of 15 m (50 ft) was used for case study 1, and a thickness of 5 m (15 ft) was used for case study 2. In both case studies, an elastic modulus of 20 GPa (3,000,000 psi) was used for the overburden.

STRESS MAPPING

In order to optimally use LAMODEL for accurate stress prediction at a given mine, the program should first be calibrated to the site-specific geomechanics based on previously observed stress conditions at that mine. One of the simplest and easiest methods to "quantify" the stress at a particular mine is to use "stress mapping." The pillar-centric stress mapping technique used here to quantify the observed stress conditions is a slight modification of the stress mapping technique originally developed for mapping areas of high horizontal stress [Mucho and Mark 1994]. For LAMODEL calibration in these case studies, the primary interest is the stress in the pillars; therefore, the primary stress indicator is the pillar rib damage, although other stress-related features, such as roof cracks or floor heave, are also noted during the stress mapping process because they can be useful indicators of stress reactions.

Stress mapping a mine area essentially consists of traveling the rooms and crosscuts in that area and carefully observing the conditions of the pillars, roof, and floor. The observed

conditions are assigned a numerical rating and indicated on a map. For the rib damage stress mapping used here, the following numerical rating criteria were applied:

0: Rib still intact with no sloughed coal, original rock dust still in place.
1: Very slight pillar sloughage, some broken coal at base of rib.
2: Slight pillar sloughage, broken coal covers one-third of rib.
3: Significant pillar sloughage, broken coal piled halfway up rib.
4: Severe pillar sloughage, broken coal piled almost to roof.
5: Rib is composed of completely broken coal at the angle of repose, pillar may be failed.

MODEL CALIBRATION

In the model calibration process, the initial material properties are systematically adjusted in subsequent runs of the model until the results correspond as closely as possible to field observations and/or empirical formulas. For the coal properties, the in situ coal strength is adjusted until the pillar stress/failure in the model matches the observed pillar behavior as represented by the stress mapping/rib rating. For the gob properties, the final modulus value is typically adjusted up or down in LAMODEL to increase or decrease the gob stress until the model gob stress matches empirical abutment angle formulas [Mark and Chase 1997] and/or field measurements and observations. For the overburden properties, the lamination thickness is typically adjusted up to provide wider abutment stresses and smaller interseam stresses or adjusted down to provide narrower abutment stresses and greater interseam stresses as dictated by the observed stress mapping.

Once the model is reasonably calibrated and realistic pillar strengths and load distributions have been established, the mechanics-based overburden behavior in the LAMODEL program can be effectively used to accurately analyze the complicated stresses and displacements associated with future complex mining scenarios. The above technique of combining empirical pillar strength and abutment load formulas with in-mine stress mapping and the analytical mechanics of a displacement-discontinuity model capitalizes on the strengths of both the empirical and analytical approaches to pillar design. The empirical formulas and observational calibration base the model on realistic behavior; the analytical mechanics allow the model to accurately consider and analyze the effects of numerous geometric and geologic variables. Using this technique, a displacement-discontinuity model can be the most practical approach for stress analysis and pillar design in complex mining situations such as multiple seams, random pillar layouts, and/or variable topography.

CASE STUDY 1

The first case study location was a multiple-seam, room-and-pillar coal mining situation in eastern Kentucky. At this location, the lower mine had been adversely affected by mining in the upper seam (see figure 1). In particular, the lower mine experienced serious ground control problems when it mined under a barrier pillar between two upper seam gobs ("Model Area" shown in figure 1). At this multiple-seam interaction site, in-mine stress mapping was used to quantify the severity of the multiseam interactions. This stress mapping was also used to calibrate a LAMODEL simulation of the area. The results of this numerical simulation provided predicted stress levels to avoid in future multiple-seam or high-cover mining.

The geology at this location is fairly typical of the southern Appalachian coal basin, with various sedimentary layers of sandstones, siltstones, shales, and numerous coal seams. The topography is very rugged, with various steep ridges and valleys that have a topographic relief of over 600 m (2,000 ft) (see figure 1). The overburden in the study area ranged from 150 to 450 m (500 to 1,500 ft), with an average of about 300 m (1,000 ft). Because of the highly variable topography at this mine, it was critical to include the topographic stress effects in LAMODEL in order to obtain accurate results.

The overlying, or upper, mine operates in the Upper Darby Seam, which typically averages about 2.0 m (6.0 ft) thick. The lower mine operates in the Kellioka Seam, which averages about 1.5 m (4.5 ft) thick in the study area. The interburden between the two seams averages about 14 m (45 ft) and consists of interbedded sandstones and shales. The core logs nearest to the study site indicate about 3.5 to 5 m (10 to 15 ft) of shale directly over the Kellioka Seam. This is then overlain by 7.5 to 10.5 m (25 to 35 ft) of interbedded sandstones and shales, with shale primarily forming the floor of the Upper Darby Seam. Both mines are room-and-pillar drift mines and use continuous miners for coal extraction. In some production sections, depending on local mining conditions, the mines remove the pillars on retreat for full extraction.

In the study area, the lower mine was forced to dogleg around an abandoned, flooded mine in the upper seam (not shown in figure 1). This dogleg forced the lower mine to develop entries under a barrier pillar between two previously mined, upper seam gobs, as shown in the detail of figure 2. Mine management anticipated increased multiple-seam stresses in this area. In an effort to safely control these higher stress levels, the mine located the critical travelway and belt entries

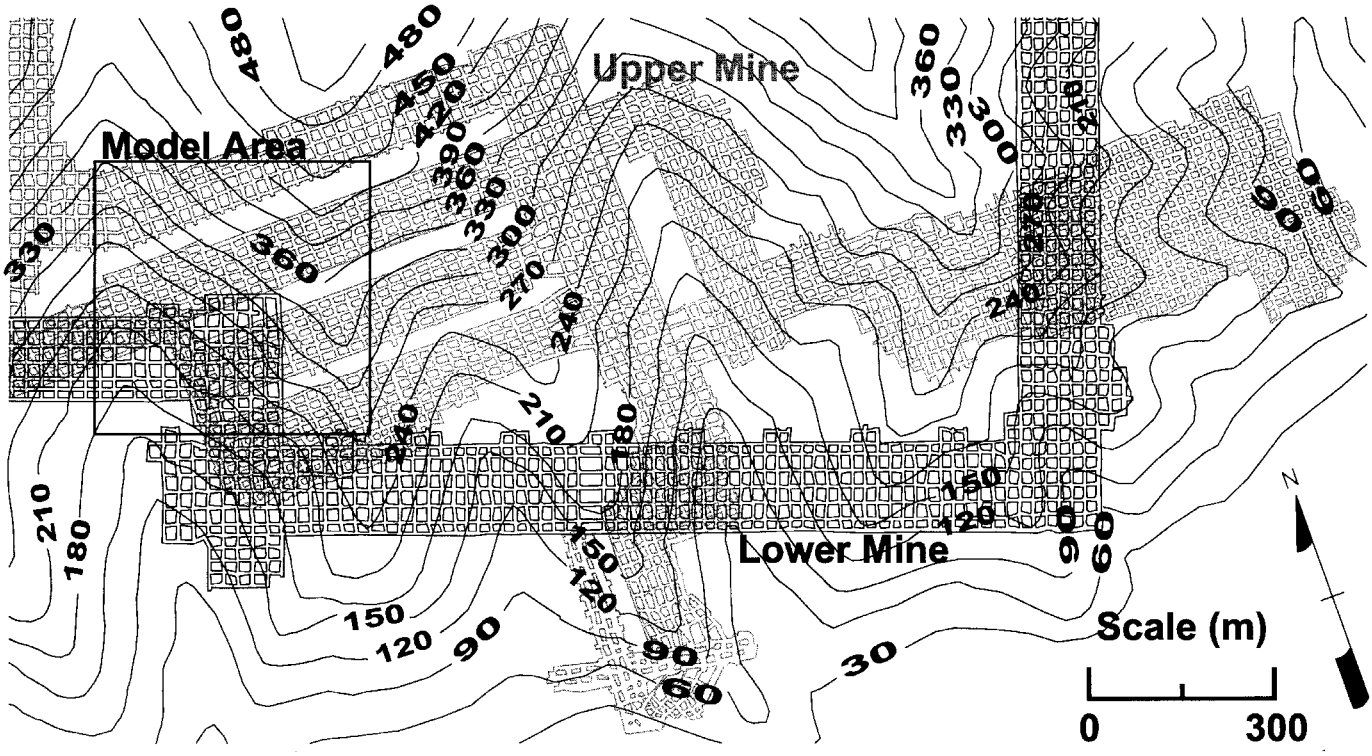

Figure 1.—Mine map for case study 1.

away from the influence of the barrier pillar and used a double row of supplemental cable bolts on 0.6-m (2-ft) centers throughout most of the travel entry under the upper seam mining. With these precautions, the mine was able to safely and efficiently mine the entries under the barrier pillar and surrounding gob. However, throughout the section, the stress effects of the overlying barrier and gob were abundantly visible, and on two occasions (in the northeast corner of the section), the mine was unable to complete crosscuts because of roof instability and poor pillar conditions.

STRESS MAPPING

In order to quantify the stress effects of the barrier pillar and gob zones on the lower seam, a detailed stress mapping of a large portion of overmined area was performed. As previously described, the amount of rib sloughing was noted on a scale of 0 to 5, and any stress-related features such as roof cracking, potting, cutting, or floor heave were also noted. The results of this stress mapping exercise are shown in figure 3*A*. In this figure, the observed condition of the pillar ribs is shown in gray scale by degree of damage; the darker shades signify increased sloughing (or stress). Also, the observed roof cracking, potting, cutting, and floor heave are indicated on the map.

Several useful observations can be made from the detailed stress mapping shown in figure 3*A*. First, the transfer of the abutment stresses from the overlying mine to the area under the barrier pillar and to the area at the ends of the pillared sections can clearly be inferred in the rib conditions of the lower mine pillars. Also, as a corollary to the interseam transfer of the

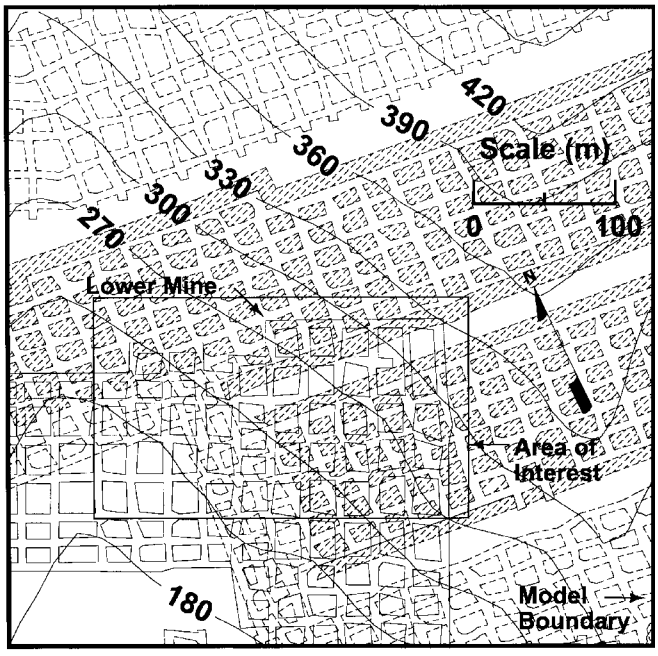

Figure 2.—Enlargement of model area for case study 1.

barrier pillar abutment stresses, the lower seam pillars under the gob areas in the upper seam show considerable stress relief. The next major observation pertains to the location and orientation of the roof tension cracks and guttering. Clearly, the tension cracks in the roof of the northeast corner of the section are situated directly under the overlying barrier pillar and are oriented parallel to the axis of this pillar. Also, the observed

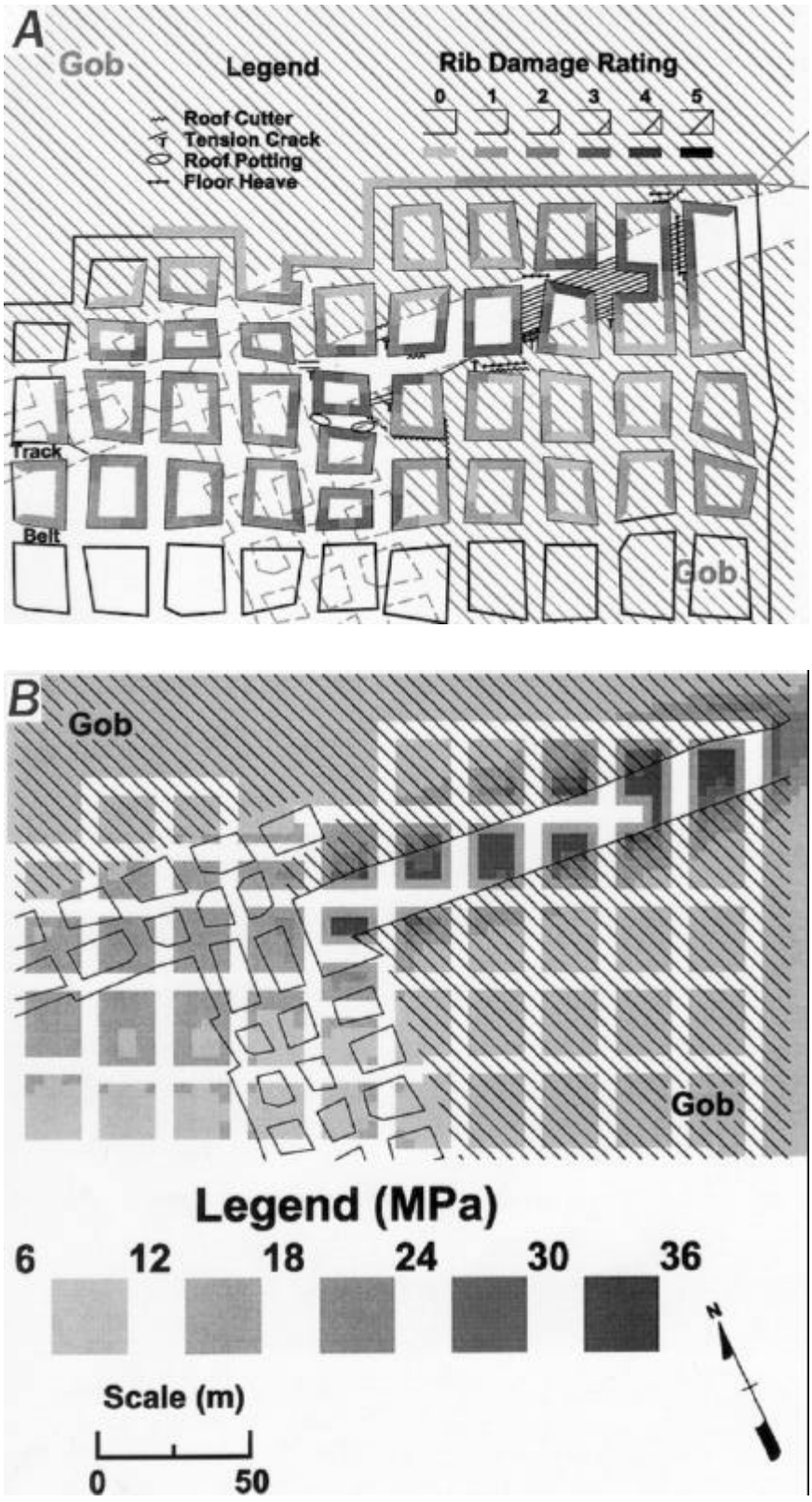

Figure 3.—Comparison between (*A*) in-mine stress mapping and (*B*) LAMODEL calculated stresses for mine 1.

compressional roof cutters are located at the edge of, or adjacent to, the overlying abutment zones and oriented parallel to these zones. This location and orientation of the tension and compression suggest that the lower mine roof is behaving like a beam that is bending into the relatively soft coal seam under the load of the barrier pillar in the upper seam. This beam scenario correctly accounts for the tension directly under the applied load and the compression adjacent to the applied load.

MODEL DESIGN

For the LAMODEL simulation of this area, the seams were discretized with 3-m (10-ft) elements in a 150-by-150 grid with the model boundary, as shown in figure 2. Symmetrical seam boundary conditions were set on all four sides, and no free-surface effects were included. The interburden was set at 14 m (45 ft), and the rock mass was simulated with a modulus of 20 GPa (3,000,000 psi) and 15-m (50-ft) thick laminations. An elastic, perfectly-plastic material was used for the coal in both seams, and the peak strength of the coal was determined from the Mark-Bieniawski pillar strength formula, as in appendix C of Heasley [1998]. Table 2 presents the coal and gob input values used in LAMODEL for this particular case study.

Also, because of the high topographic relief at the site, the topography was discretized with 15-m (50-ft) elements for an area extending 300 m (1,000 ft) beyond the limits of the displacement-discontinuity grids. The importance of including the topographic stress effects in the model is evident in figure 4, which shows the topographic stress at the level of the lower mine. It is interesting to note in this figure the amount to which the topographic stress is "smoothed" with depth compared to the original topography. Also, it is evident that the overburden stress changes about 3 MPa (450 psi) in traversing from the southwest to the northeast corner of the pillars in the study area. This difference in overburden stress could very well account for the increased mining difficulties at the northeast corner of the section.

MODEL CALIBRATION AND ANALYSIS

Very little work was required for calibrating the LAMODEL simulation to the observed stress mapping. In both seams, the original Mark-Bieniawski pillars strengths and the initial overburden modulus and lamination thickness provided a good fit to the observed pillar behavior (see figure 3). The only parameter that was ultimately manipulated was the modulus of the gob material (see table 2). This modulus was adjusted to provide a peak gob stress in the range of 40% to 60% of in situ stress, a reasonable range for a 90-m (300-ft) wide gob in 300 m (1,000 ft) of cover [Mark and Chase 1997]. A number of variations in pillar strength, overburden modulus, and lamination thickness were investigated, and the simulation results varied a little. However, the initial parameter values with the adjusted gob modulus provided a reasonably optimum fit to the observational stress mapping.

Table 2.—Coal and gob parameters for case study 1

COAL ELEMENTS: UPPER MINE		
Element	Peak stress, MPa	Peak strain
A (core)	85.9	0.04152
B	56.1	0.02712
C	38.3	0.01992
D (rib)	11.4	0.00552
COAL ELEMENTS: LOWER MINE		
Element	Peak stress, MPa	Peak strain
A (core)	113.2	0.05472
B	73.5	0.03552
C	53.6	0.02592
D (rib)	13.9	0.00672
GOB ELEMENTS		
Initial modulus, MPa	Final modulus, MPa	Final stress, MPa
6.2	110	27.6

The calculated pillar stresses from the final calibrated LAMODEL run are shown in figure 3*B*. These modeled stresses correlate extremely well with the stress mapping in figure 3*A*. The high stresses under the barrier pillar are evident in the model results; the area of stress relief under the gob is also shown. Even the intermediate stress levels under the overlying pillars and solid coal in the southwest corner of the model closely match the observed pillar stress mapping. A few more details of the modeled stress output are shown in figure 5, where the isolated single-seam stress and just the interseam stress are displayed. In this figure, the effect of the overlying barrier pillar can be clearly seen. In particular, the maximum single-seam stress on the pillars (figure 5*A*) of around 15 MPa (2,200 psi) is seen to increase to over 36 MPa (5,200 psi) with the addition of the barrier pillar stress (figures 5*B* and 5*C*). Also, it is interesting to note the increased abutment stress in the northeast corner of the section (figure 5*C*), presumably due to the increasing overburden and the increasing distance from the upper panel boundaries. A stress relief of about 7 MPa (1,000 psi) under the gob areas is also shown in figure 5*C*.

For the mine management, this stress modeling using LAMODEL, in conjunction with good in-seam correlations with stress mapping, provided valuable background information for future multiple-seam mine planning. In this case study, a calculated multiseam stress concentration of about 15 MPa (2,200 psi) with pillar stresses of 35 MPa (5,200 psi) at this site caused sufficient roof instability to prohibit the mine from driving two crosscuts. Therefore, it seems that the 15-MPa stress concentration (35-MPa pillar stress) is close to an upper limit for successful entry development at this mine. The mine can use this calculated limit in conjunction with future modeling in order to lay out future room-and-pillar panels influenced by overlying workings.

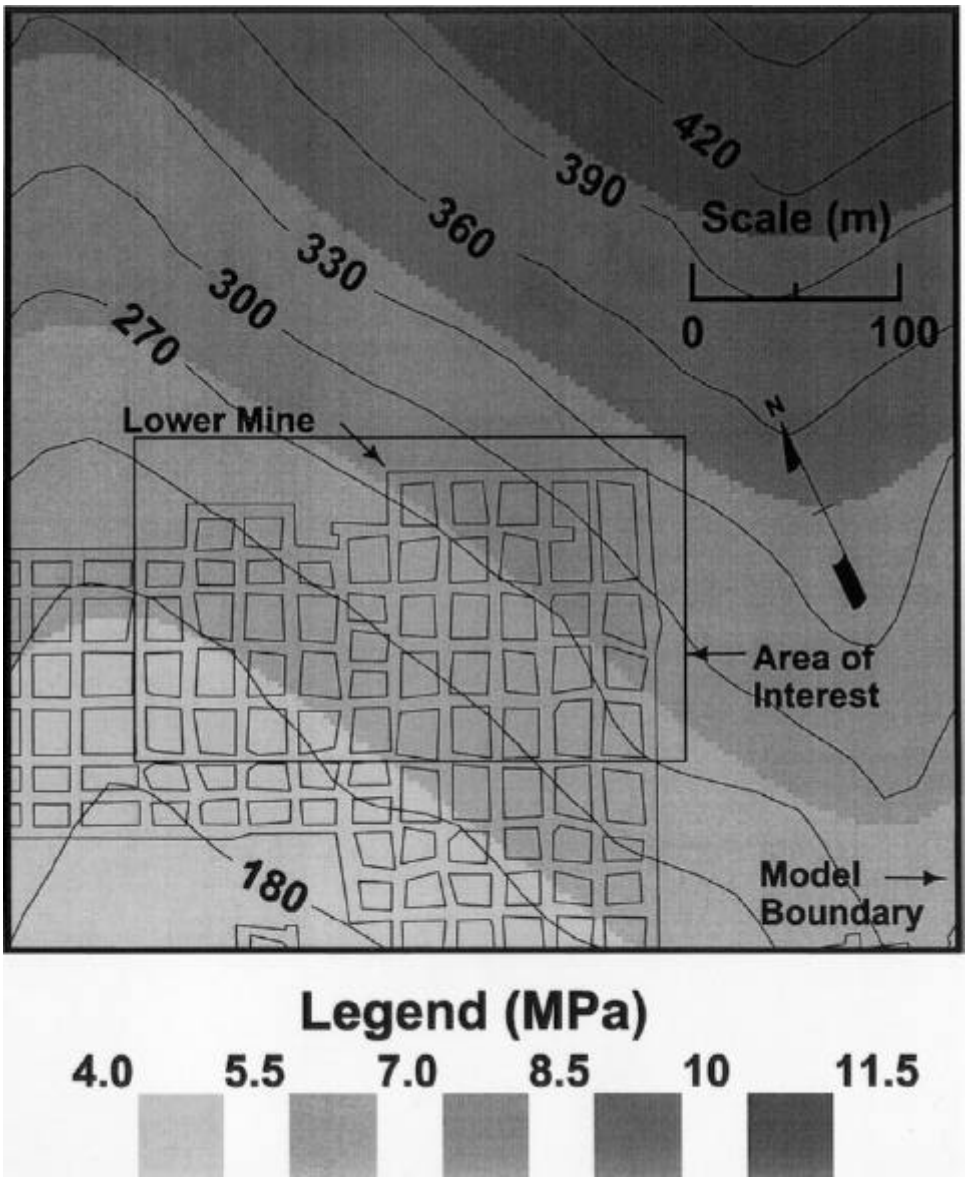

Figure 4.—Calculated topographic stress for case study 1.

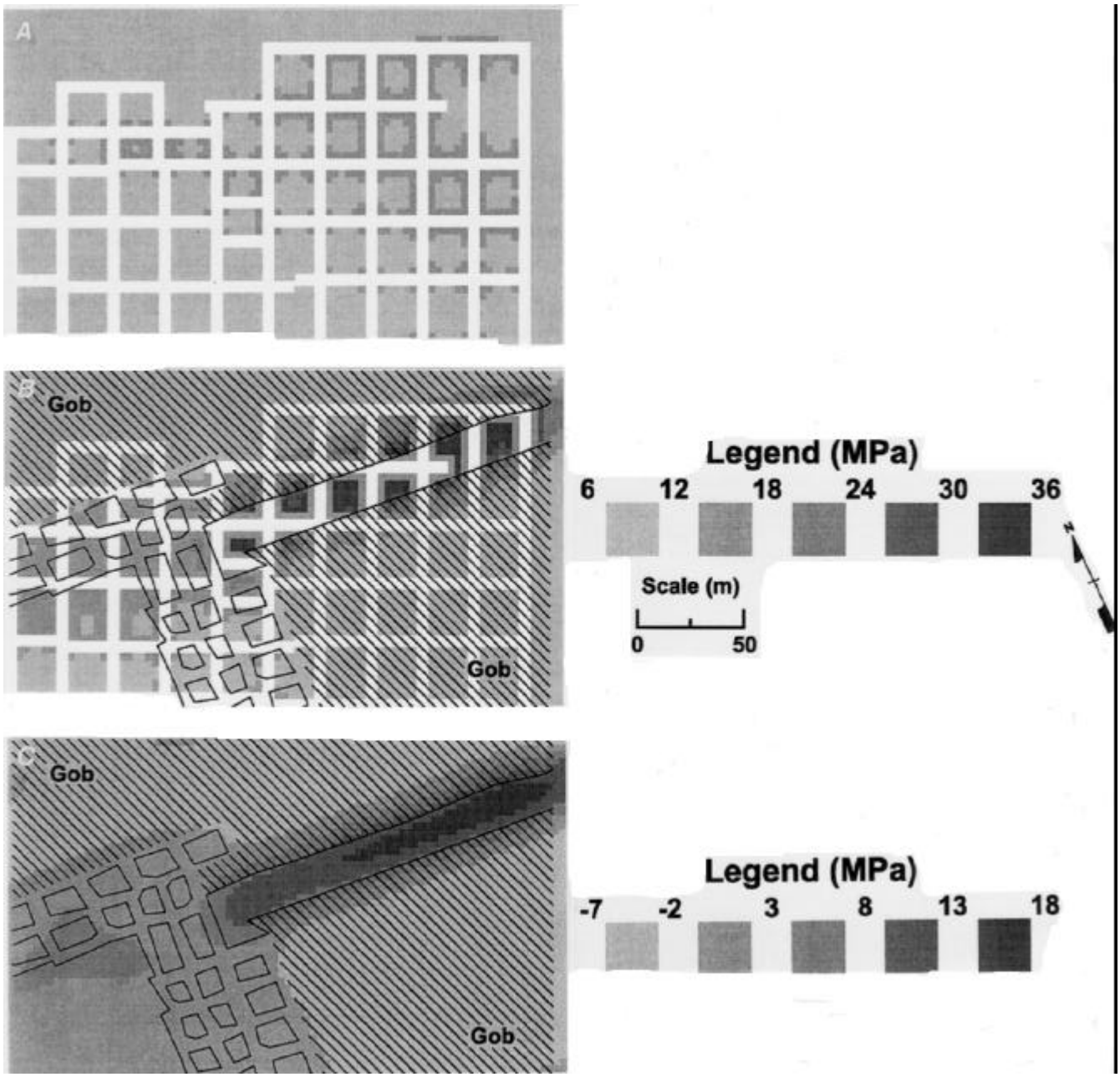

Figure 5.—The LAMODEL stress output for case study 1. *A*, Single-seam stress; *B*, multiple-seam stress; *C*, additional stress from upper seam.

CASE STUDY 2

The second study site was a longwall mine located in Greene County, PA, and operating in the Sewickley Seam. This mine is underlain by an abandoned room-and-pillar operation in the Pittsburgh Seam. The primary problem at this site was the transfer of multiple-seam stress from the lower mine. Yielding of smaller pillars and the subsequent transfer of their load to larger pillars in the lower seam apparently caused increases in vertical stress in the upper seam that were noticed during development of the headgate entries (see figure 6). Severe pillar spalling and poor roof conditions were experienced when mining the headgate over these large pillars in the lower seam (figure 7). Mine management was concerned that these underlying abutment pillar stresses would continue to be a problem farther inby in the headgate and also in the longwall panel because there were several areas in the lower seam where similar pillar conditions seemed to exist.

In the study area, the overburden above the Sewickley Seam ranges from 150 to 280 m (500 to 910 ft) and consists predominantly of interbedded shales and sandstones. The interburden between the Sewickley and Pittsburgh Seams ranges from 27 to 30 m (90 to 100 ft) thick and consists of interbedded shales and limestones. The average mining heights of the Sewickley and Pittsburgh Seams are 1.5 m (5 ft) and 1.8 m (6 ft), respectively. The immediate roof of the Sewickley Seam is composed of a jointed dark sandy shale that ranges from 3 to 4.5 m (10 to 15 ft) thick and is overlain by a competent limey shale. The immediate floor of the Sewickley Seam is composed of a 1.2-m (4-ft) thick dark limey shale underlain by a competent limestone unit.

STRESS MAPPING

Figure 6 shows the overlay of the lower seam workings on the upper seam longwall panel and the area of the headgate where the stress mapping and model calibration were conducted. As described earlier, the process of calibration involved the use of stress mapping to assign a rating from 0 to 5 based on the observed pillar rib conditions. The first 600 m (2,000 ft) of the headgate entries, where problems first occurred (see figure 6), were traversed and assigned rating numbers based on the observed conditions. Figure 7*A* shows the rib damage rating assigned to each rib in this area of the headgate.

MODEL DESIGN AND CALIBRATION

Once the stress mapping was complete, LAMODEL calibration was initiated. For calibration purposes, the "Stress Mapped Area" shown in figure 6 was discretized with 3-m (10-ft) elements with a 90-by-200 grid. Symmetrical boundary conditions were set on all four sides, and no free-surface effects were included. The interburden was set at 27 m (90 ft), and the rock mass was simulated with a modulus of 20 GPa (3,000,000 psi) and 5-m (15-ft) thick laminations. The overburden above the lower mine in this area ranged from 180 to 300 m (600 to 1,000 ft). Due to this variable topography, the topographic stress effects were included in LAMODEL in order to obtain accurate overburden stress results.

Based on the observed stress mapping, model calibration was conducted under the assumption that the smaller pillars (<10.5 m (<35 ft) wide) in the lower mine had essentially yielded and transferred their load to nearby larger pillars. Therefore, in the first step of the calibration process, the coal strength in the lower mine model was adjusted until the pillars showed this observed behavior. Initially, using the elastic-plastic implementation of the Bieniawski formula, as previously explained, an in situ coal strength of 6.2 MPa (900 psi) was used to calculated peak stress and strain values for each coal element, and the initial calibration model was run. In this initial model, the coal in the lower mine was too strong and did not show the desired yielding in the smaller pillars. Therefore, in order to obtain the desired small pillar yielding and subsequent stress transfer to the larger pillars, the in situ coal strength in the lower seam was gradually decreased to 4.2 MPa (600 psi).

With the in situ coal strength of 4.2 MPa (600 psi) in the lower seam and the original coal strength of 6.2 MPa (900 psi) in the upper seam, the model correlated very well with the rib damage rating from the stress mapping. The rib damage rating is in gray scale in figure 7*A*; the results from the model are in a comparative gray-scale plot in figure 7*B*. Clearly, the model pillars with high rib stress correlate well with the pillars with high damage ratings. It can be observed in figure 6 that these high rib stresses occur over the large pillars located in the lower mine in conjunction with overburden that exceeds 250 m (870 ft). The final coal and gob properties used in LAMODEL for the upper and the lower mine are presented in table 3.

Table 3.—Coal and gob parameters for case study 2

COAL ELEMENTS: UPPER MINE		
Element	Peak stress, MPa	Peak strain
A (core)	102.3	0.04944
B	66.5	0.03216
C	48.7	0.02352
D (rib)	12.9	0.00624
COAL ELEMENTS: LOWER MINE		
Element	Peak stress, MPa	Peak strain
A (core)	56.8	0.02747
B	36.9	0.01787
C	27.0	0.01307
D (rib)	7.2	0.00347
GOB ELEMENTS		
Initial modulus, MPa	Final modulus, MPa	Final stress, MPa
6.2	138	27.6

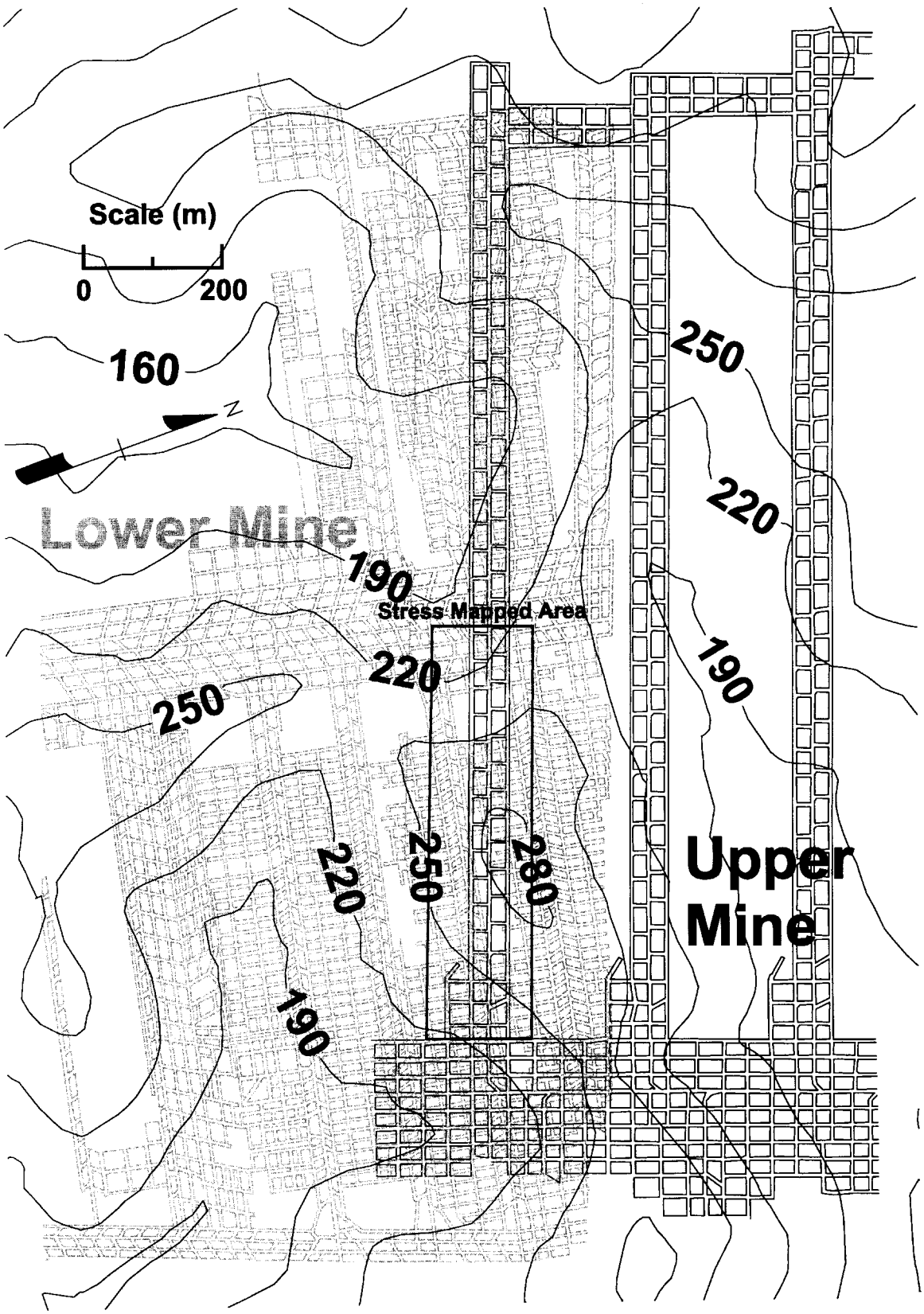

Figure 6.—Mine map for case study 2.

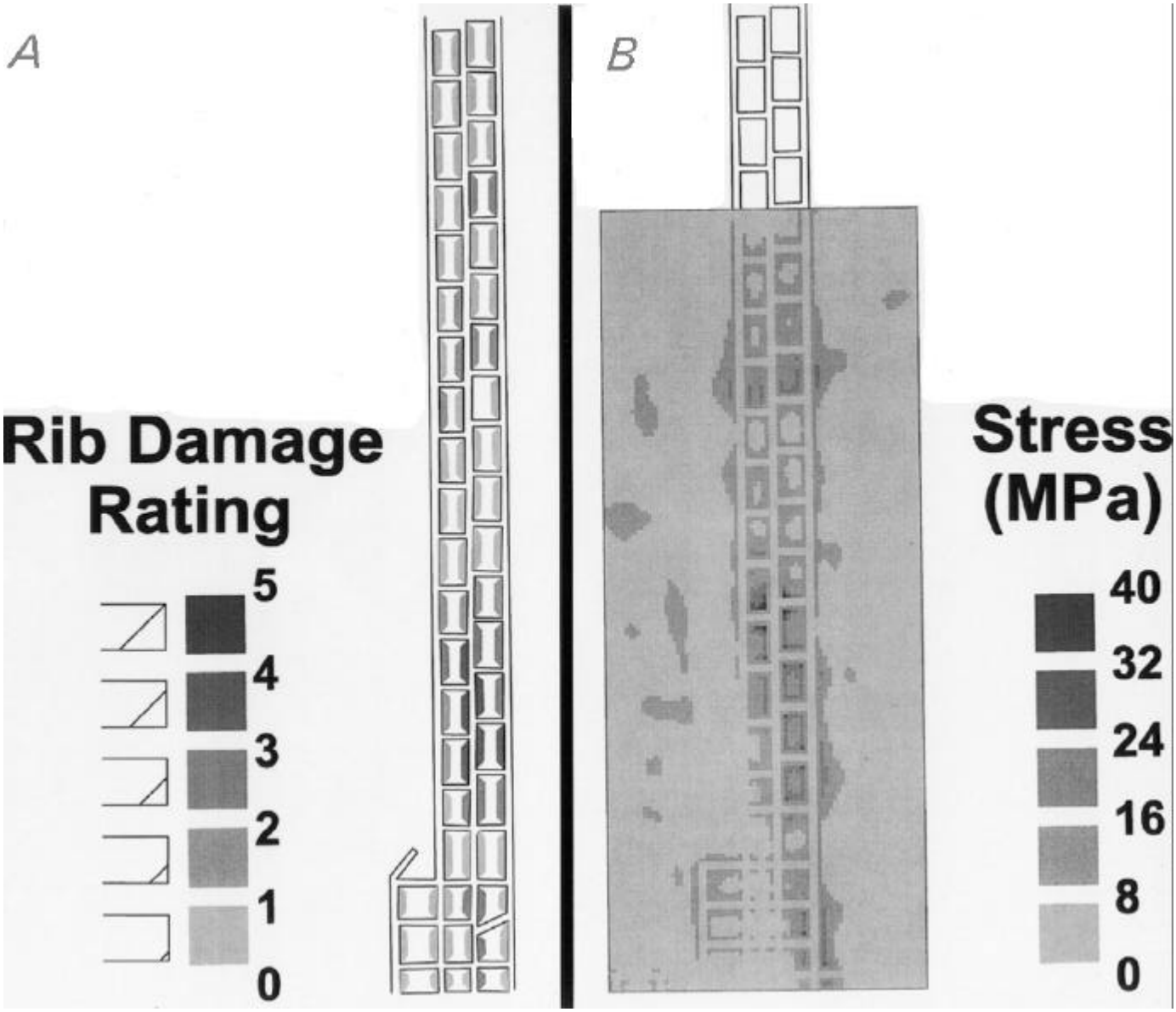

Figure 7.—Comparison between in-mine stress mapping and LAMODEL calculated stresses. *A*, rib damage rating; *B*, stress (MPa).

STRESS PREDICTION FOR MINE PLANNING

With material properties calibrated from observed stress conditions in the mine, additional LAMODEL analyzes were created and run in order to predict areas of potential problems within the remaining headgate and the future longwall panel. Figure 8 shows two areas of the headgate and longwall panel that were modeled using optimized properties from the calibration process. These gray-scale plots show the interseam stress, which is the additional stress on the upper mine due to the lower seam mining. In this figure, zone 1 covers the upper (inby) part of the headgate panel and the first 365 m (1,200 ft) of the longwall panel; zone 2 covers the lower part of the headgate (where the stress problems were first noticed) and the last (outby) 330 m (1,100 ft) of the longwall panel. In these two zones, the lower mine pillar conditions and the overburden depths appeared similar; therefore, the poor pillar conditions encountered in zone 2 were expected in zone 1.

However, when comparing the interseam stress between these two zones as shown in figure 8, it is obvious that the stress in zone 2 is considerably greater than that in zone 1. Closer investigation reveals two primary reasons for this. First, the maximum depth over the gate roads and panel in zone 2 is over 280 m (920 ft); in zone 2, the maximum depth is just over 250 m (870 ft). Second, when examining the model output for the lower mine, there seems to be less pillar yielding in zone 1 than in zone 2. In figure 6, it can be seen that the smaller pillars in zone 1 are dispersed among larger pillars and have widths >12 m (>40 ft), whereas in zone 2, there is a large area of pillars with widths <10.5 m (<35 ft). The larger, more dispersed small

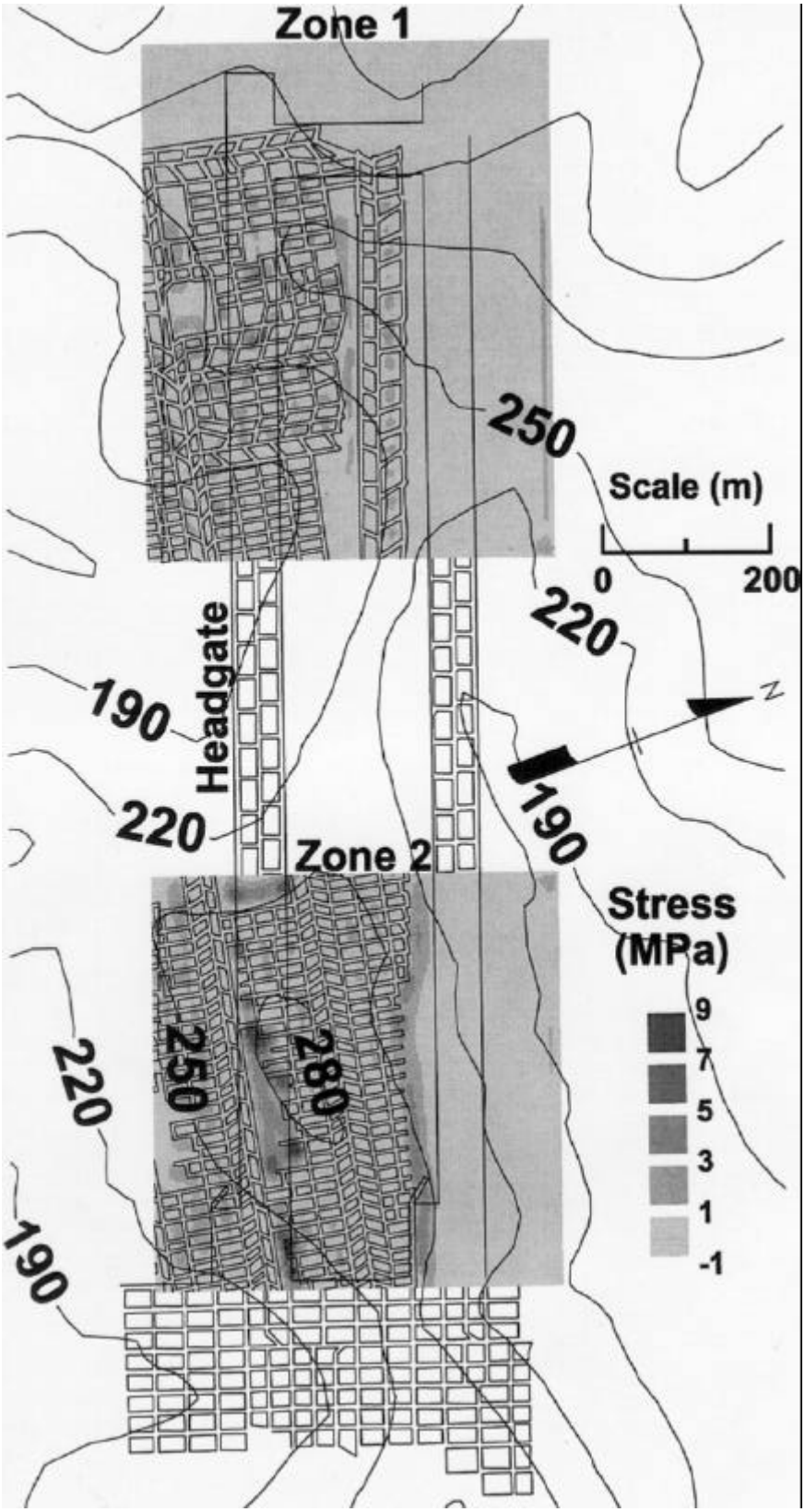

Figure 8.—Interseam stress for zones 1 and 2.

pillars in zone 1 suffer less pillar yielding and therefore cause less load transfer (or interseam stress) on the upper mine (see figure 8). During headgate development in zone 1, no pillar problems were encountered. Thus, the calibrated model successfully predicted the reduced stress conditions in the headgate of zone 1.

The mine management was also concerned about the multiple-seam stresses adversely affecting the retreating longwall panel. In particular, a large, irregularly shaped barrier pillar in the lower mine is superimposed under the center line of the initial half of the longwall panel in zone 1 (see figure 8). However, the interseam stress calculated by the model from this barrier pillar reaches only about 3 MPa (450 psi). When the panel was mined, this slightly increased face stress presented very little problem. Some slight spalling was present on the face during the extraction, but overall face conditions were generally good and no severe ground control problems were evident.

However, in the lower part of the panel near the headgate location where poor ground conditions were first encountered (see zone 2, figure 8), an area of interseam stress up to 9 MPa (1,300 psi) is evident in the panel. Because of the underlying barrier pillar, the mine anticipated difficult face conditions in this area. Indeed, when the longwall face reached this area, ground control problems that included severe face spalling and poor roof condition in the headgate entries were encountered. In fact, the stress interaction with the lower seam was severe enough to stop the longwall face about 15 m (50 ft) short of the longwall recovery chute and make recovery of the supports difficult.

When comparing conditions in zone 1 with those of zone 2, there seems to be a very fine line in the occurrence of ground control problems in the upper seam depending on the overburden depth and the pillar size in the lower seam. Problems were more likely to occur when the depth of cover over the Sewickley Seam exceeded 250 m (820 ft) and when large areas of narrow pillars (<10.5 m (<35 ft) wide) in the lower seam were located adjacent to a larger barrier pillar. These conditions caused yielding of the narrow pillars and the shedding of their load to the adjacent larger pillar. This concentrated abutment stress was then transferred to the upper mine, resulting in poor ground conditions in areas of the headgate entry and longwall panel. Throughout this case study, the calibrated LAMODEL program successfully predicted the high stress areas in advance of mining.

CONCLUSIONS

The primary purpose of the case studies presented in this paper was to validate the new LAMODEL boundary-element program and investigate its utility for stress modeling in mine planning. Based on the comparisons between the stress mapping and the model results for the two case studies, it seems that the LAMODEL program can be calibrated to produce good correlations with the observed stresses. In addition, once realistic pillar strengths and load distributions were established by calibration, the mechanics-based overburden behavior in LAMODEL effectively analyzed the complicated stresses and displacements associated with the complex multiple-seam mining scenarios and successfully predicted upcoming high stress conditions in advance of mining for preventive action by mine management. In case study 1, a calculated multiseam stress concentration of around 15 MPa (2,200 psi) with pillar stresses of 35 MPa (5,200 psi) seemed to be an upper limit for successful entry development at this mine. Similarly, in case study 2, a calculated multiple-seam stress concentration of 9 MPa (1,300 psi) produced severe face spalling and poor roof conditions in the headgate entries, whereas a 3-MPa (450-psi) stress concentration was barely noticeable.

A secondary goal was to present a fairly streamlined, systematic methodology for developing initial material properties and then calibrating these properties to field observations. Initially, the critical material properties (coal, gob, and rock mass) are developed using a combination of laboratory research, empirical formulas, and experience. Then, in the calibration process, a previously mined area is "stress mapped" by quantifying the observed pillar and strata behavior using a simple numerical rating system. Finally, the initial material properties are systematically adjusted in subsequent runs of the model until the results provide the best correlation between the predicted stresses and the observed underground stress rating. This methodology of combining empirical pillar strength and abutment load formulas with in-mine stress mapping and the analytical mechanics of a displacement-discontinuity model capitalizes on the strengths of both the empirical and analytical approaches to pillar design to provide a practical technique for mine planning in difficult situations.

REFERENCES

Heasley KA [1998]. Numerical modeling of coal mines with a laminated displacement-discontinuity code [Dissertation]. Golden, CO: Colorado School of Mines, Department of Mining and Earth Systems Engineering.

Kanniganti RS [1993]. Interactive prediction software for underlying multi-seam design [Thesis]. Blacksburg, VA: Virginia Polytechnic Institute and State University, Department of Mining and Minerals Engineering.

Karabin GJ, Evanto MA [1999]. Experience with the boundary-element method of numerical modeling to resolve complex ground control problems. In: Proceedings of the Second International Workshop on Coal Pillar Mechanics and Design. Pittsburgh, PA: U.S. Department of Health and Human Services, Public Health Service, Centers for Disease Control and Prevention, National Institute for Occupational Safety and Health, DHHS (NIOSH) Publication No. 99-114, IC 9448.

Mark C [1992]. Analysis of longwall pillar stability (ALPS): an update. In: Proceedings of the Workshop on Coal Pillar Mechanics and Design. Pittsburgh, PA: U.S. Department of the Interior, Bureau of Mines, IC 9315, pp. 238-249.

Mark C, Barton TM [1997]. Pillar design and coal strength. In: Proceedings - New Technology for Ground Control in Retreat Mining. Pittsburgh, PA: U.S. Department of Health and Human Services, Public Health Service, Centers for Disease Control and Prevention, National Institute for Occupational Safety and Health, DHHS (NIOSH) Publication No. 97-122, IC 9446, pp. 49-59.

Mark C, Chase FE [1997]. Analysis of retreat mining pillar stability (ARMPS). In: Proceedings - New Technology for Ground Control in Retreat Mining. Pittsburgh, PA: U.S. Department of Health and Human Services, Public Health Service, Centers for Disease Control and Prevention, National Institute for Occupational Safety and Health, DHHS (NIOSH) Publication No. 97-122, IC 9446, pp. 17-34.

Mucho TP, Mark C [1994]. Determining horizontal stress direction using the stress mapping technique. In: Peng SS, ed. Proceedings of the 13th International Conference on Ground Control in Mining. Morgantown, WV: West Virginia University, pp. 277-289.

Pappas DM, Mark C [1993]. Behavior of simulated longwall gob material. Pittsburgh, PA: U.S. Department of the Interior, Bureau of Mines, RI 9458.

Zipf RK Jr. [1992]. MULSIM/NL theoretical and programmer's manual. Pittsburgh, PA: U.S. Department of the Interior, Bureau of Mines, IC 9321.